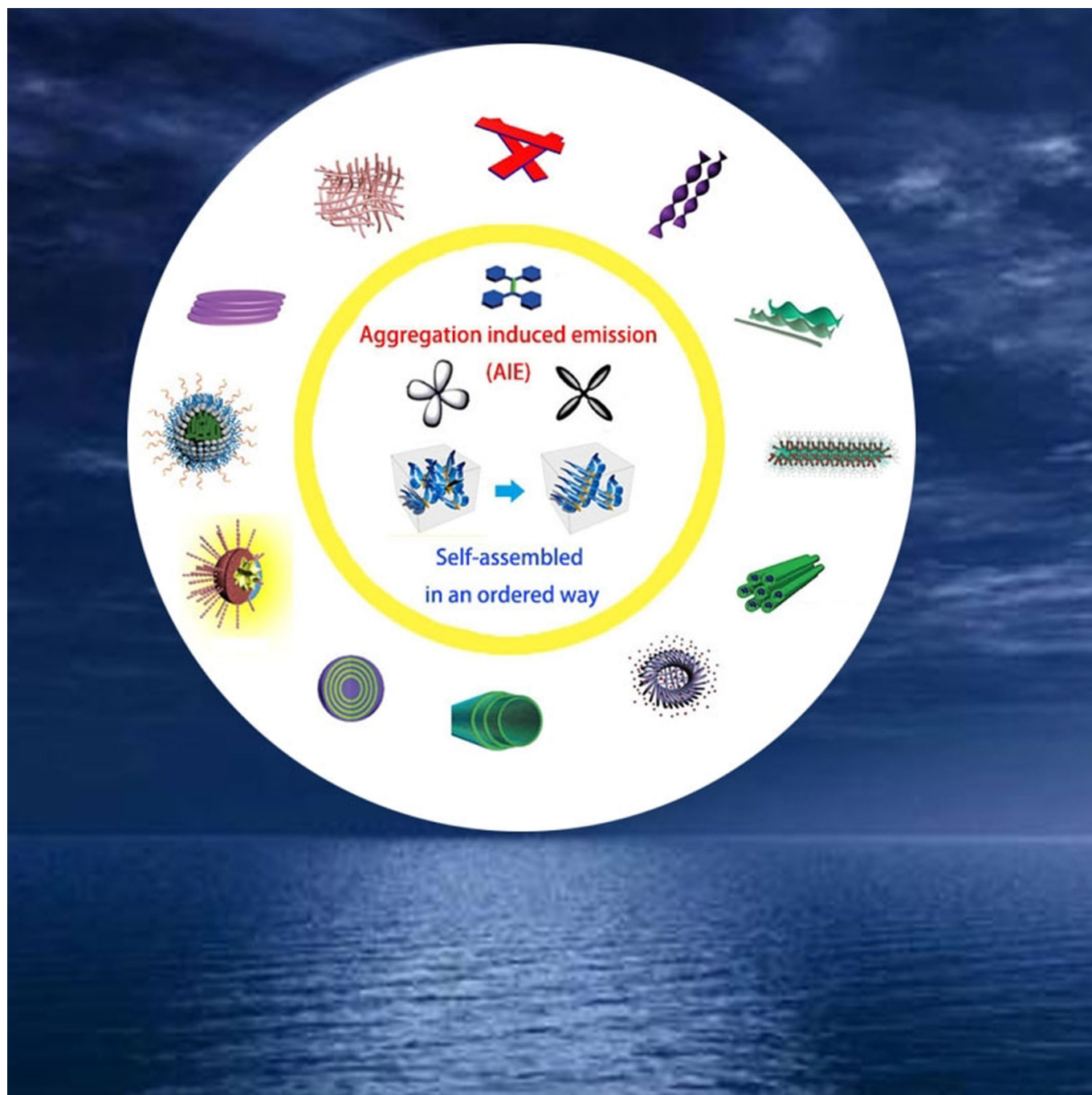


Self-Assembly of Aggregation-Induced-Emission Molecules

Tongyue Wu, Jianbin Huang, and Yun Yan*^[a]



Abstract: The last decade has witnessed rapid developments in aggregation-induced emission (AIE). In contrast to traditional aggregation, which causes luminescence quenching (ACQ), AIE is a reverse phenomenon that allows robust luminescence to be retained in aggregated and solid states. This makes it possible to fabricate various highly efficient luminescent materials, which opens new paradigms in a number of fields, such as imaging, sensing, medical therapy, light harvesting, light-emitting devices, and organic electronic devices. Of the various important features of AIE molecules, their self-assembly behavior is very attractive because

the formation of a well-defined emissive nanostructure may lead to advanced applications in diverse fields. However, due to the nonplanar topology of AIEgens, it is not easy for them to self-assemble into well-defined structures. To date, some strategies have been proposed to achieve the self-assembly of AIEgens. Herein, we summarize the most recent approaches for the self-assembly of AIE molecules. These approaches can be sorted into two classes: 1) covalent molecular design and 2) noncovalent supramolecular interactions. We hope this will inspire more excellent work in the field of AIE.

Introduction

Light-emitting materials with tunable luminescent properties are of tremendous interest; many research and review papers have focused on this topic.^[1] However, due to aggregation-caused quenching (ACQ), conventional organic fluorescent molecules can only be emissive in dilute solution, which greatly limits their applications in solid luminescent materials. Many efforts have been made to overcome this problem, such as attaching branched chains or bulky cycles^[2] or blending them with polymers with a high glass-transition temperature,^[3] but unfavorable results were obtained.

The phenomenon of aggregation-induced emission (AIE), discovered by Tang et al. in 2001,^[4] offers another way to solve this problem. They developed a new class of molecules that are nonemissive in solution but become strongly luminescent upon aggregation. This abnormal fluorescent behavior is ascribed to the restriction of internal rotation (RIR), aggregation-induced planarization, and the formation of J-aggregates in some cases.^[5] After years of research, many marvelous molecules that exhibit AIE effects have been designed.^[6]

Molecular self-assembly is the oriented association of molecules into nano- or microscopic structures through noncovalent interactions.^[7] AIE molecules offer great advantages as ideal building blocks for the construction of luminescent micro-/nanostructures because of their high fluorescence efficiency in the solid state and variable emission colors.^[8] Due to their unique properties, AIE molecules can be designed as a new kind of functional material that has broad applications in fields such as biology, the environment, materials, pharmacy, and agriculture.

However, classical AIE molecules are difficult to assemble into ordered assemblies spontaneously because they have nonplanar topology that can hardly pack in an orderly way. To date, there are two main approaches to promote the self-assembly of AIE molecules: 1) through molecular design, which requires a covalent link between a proper organic group and the AIE moiety to promote aggregation or 2) through noncovalent interactions, such as ionic binding, coordination, host-guest interactions, π - π stacking, or hydrogen bonding, to embed the AIEgens in a self-assembled ensemble.^[7] Herein, we introduce literature results that have achieved the self-assembly of AIEgens, with the hope of expanding the direction of self-assembly of AIE molecules. Only the self-assembly of organic AIE molecules is covered, whereas inorganic clusters that display AIE effects are not covered.


General design principles for the self-assembly of AIEgens

AIEgens feature nonplanar structures, such as 1) propeller-shaped molecules (Figure 1a), 2) butterfly or V-shaped molecules (Figure 1b), or 3) rotatable linear molecules (Figure 1c). It is this nonplanar topology that hinders the molecules from packing closely to form well-defined structures. Therefore, the central problem in enhancing the self-assembly ability of AIE molecules is to promote intermolecular interactions, such as π - π stacking, hydrogen bonding, van der Waals forces, and hydrophobic effects. This can be achieved either through molecular design or through supramolecular interactions.

Endowing AIE molecules with self-assembly ability through molecular design

Molecular design is a powerful approach that may lead to the desired material performance, which is also true in the promotion of self-assembly ability. With proper molecular design, intermolecular interactions, such as π - π stacking, hydrogen bonding, van der Waals forces, and hydrophobic effects, can be strengthened, which is beneficial for orderly packing of the molecules.

[a] T. Wu, Prof. J. Huang, Prof. Y. Yan
Beijing National Laboratory for Molecular Sciences (BNLMS)
State Key Laboratory for Structural Chemistry of Unstable and Stable Species
College of Chemistry and Molecular Engineering
Peking University
Beijing 100871 (P. R. China)
E-mail: yunyan@pku.edu.cn

 The ORCID identification number(s) for the author(s) of this article can be found under:
<https://doi.org/10.1002/asia.201801884>.

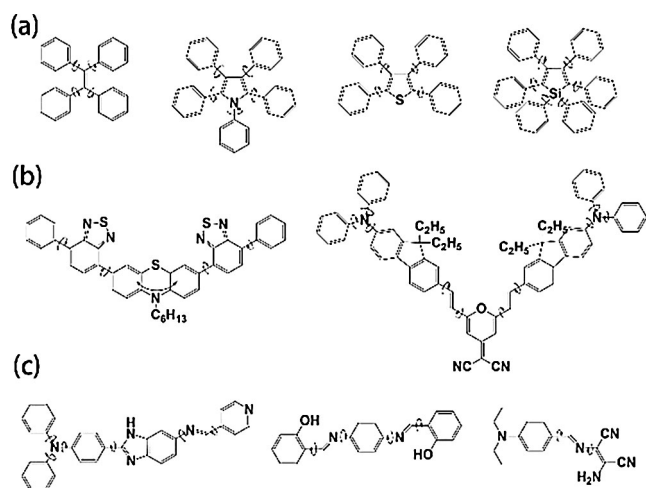


Figure 1. Typical molecular motifs that display aggregation-induced emission (AIE):^[9] a) propeller-shaped, b) V-shaped, and c) linear-shaped AIE motifs, respectively.

Enhanced hydrophobic effect

Hydrophobic, or solvophobic, effects are the simplest driving force in molecular self-assembly. Only a sufficiently strong hydrophobic effect can lead to well-defined self-assembled structures in polar media. In this context, organic groups of different structures are covalently attached to AIE cores.

Attaching long alkyl chains to AIEgens

Long alkyl chains are known to have a strong tendency to self-assemble through zigzag packing in polar media, especially water.^[10] Therefore, attaching long alkyl chains to the AIEgens is a simple option to promote their self-assembly ability.

A typical example is the AIE molecules designed by Bhosale et al. They attached four alkyl chains to each phenyl group of a tetraphenylethene (TPE) core through amide linkages.^[11] Chiral tubes were formed by these TPE derivatives. The hydrophobic effect brought about multiple cooperative supramolecular interactions that drove the formation of these chiral tubes:^[11a] 1) π - π interactions between the aromatic TPE cores, 2) long alkyl chains on the periphery of the TPE optimized the dispersive and van der Waals interactions, and 3) hydrogen bonding through amide functional groups. Together, these interactions prevented crystallization and induced the directional growth of a twisted superstructure (Figure 2a). Interestingly, they also found that odd or even numbers of carbon atoms led to opposite chiral superstructures, with right-handed supramolecular structures produced with even-numbered carbon chains and left-handed supramolecular structures with odd-numbered ones.^[11b] This is because the different alkyl chain length produced a geometric difference in alignment to maximize the van der Waals interactions (Figure 2b).

Because the long alkyl chains have a very strong hydrophobic effect and the AIE groups are also hydrophobic, the number of alkyl chains needed to create a self-assembled AIEgen structure is not necessarily that large. For example,

Song et al.^[12] designed a bola-shaped amphiphile by attaching two alkyl pyridine salts to opposite arms of the TPE moiety (Figure 3a). This compound is able to self-assemble into flake-like structures at the critical micelle concentration (CMC; Figure 3b). At higher concentrations, an elongated flake-like structure developed (Figure 3c). The nanometer-sized particles display strong emission ability, and shows good water solubility and biocompatibility, which are very promising features for cell labeling and mapping.

Recently, Zhao and Tang et al. reported that changes to the alkyl chain length can be an approach to manipulate the self-assembly of AIEgens.^[13] They synthesized a series of pyridinium-functionalized TPE salts (TPEPy) with different alkyl chains (Figure 4). As the alkyl chain length was increased, the self-assembled structure changed from microplates to microrods, and the emission color was blueshifted from red to green. Microplates were formed with the shortest alkyl chain (TPEPy-1),

Tongyue Wu is a graduate student at Peking University, under the guidance of Yun Yan and Jianbin Huang. She obtained her bachelor's degree at the same university in 2018. Her study focuses on metallosupramolecular assemblies and their related applications.



*Jianbin Huang obtained his bachelor's (1987), master's (1990), and PhD (1993) degree at Peking University, China. After a postdoctoral study at the same university, he was nominated as an associate professor in 1995, as a full professor in 2001, and was awarded "Outstanding Young Scientist of China" in 2004. His main research interests include soft self-assembly of amphiphiles and one-dimensional nanomaterials synthesized by using soft templates. He is currently the senior editor of *Soft Matter*, and also the board editor of *Langmuir*.*



*Yun Yan earned her Ph.D. degree from Peking University in 2003. She conducted her postdoctoral work at Bayreuth University, Germany, under Prof. Heinz Hoffmann and at Wageningen University, the Netherlands, under Prof. Martien A. Cohen Stuart. She joined Peking University in 2008, and was selected for the New Century Training Program for the Talents by the State Education Commission of China in 2009, awarded as "Outstanding Young Professor of Colloid Science of China" in 2013, and was the winner of the Outstanding Youth Science Foundation, Natural Science Foundation of China (NSFC, 2014). Her interest is in the methodology of molecular self-assembly. Currently, she is serving on the advisory board of *ACS Applied Materials & Interfaces*.*



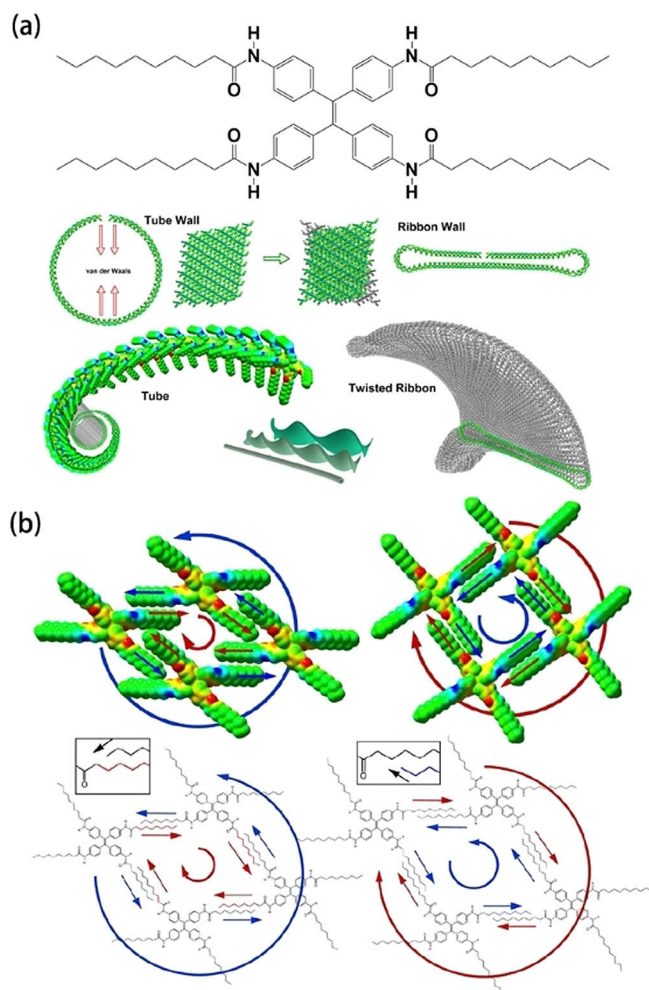


Figure 2. a) Right-handed helical superstructures from alkyl-TPE. b) Illustration of prochiral molecules arranged in opposite directions, with left- and right-handed self-assembly.^[11]

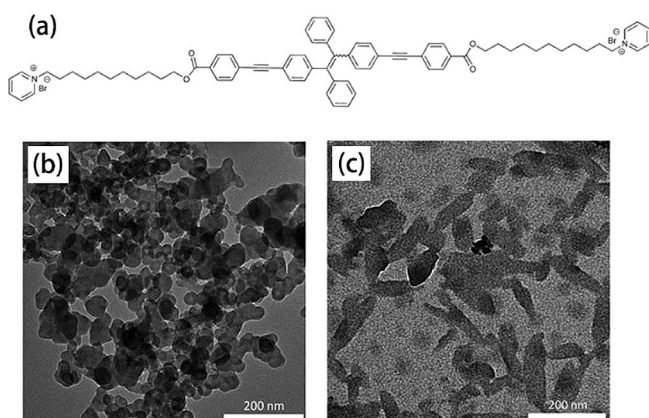


Figure 3. a) Molecular structure of a TPE-containing bola-amphiphile. b, c) TEM image of the assemblies at concentrations of 5×10^{-6} and $1 \times 10^{-3} \text{ mol L}^{-1}$, respectively.^[12]

and consisted of loosely packed molecules. This loose molecular arrangement could be influenced by NO_3^- and ClO_4^- ions in aqueous media, and thus displayed a fluorescence “turn-on”

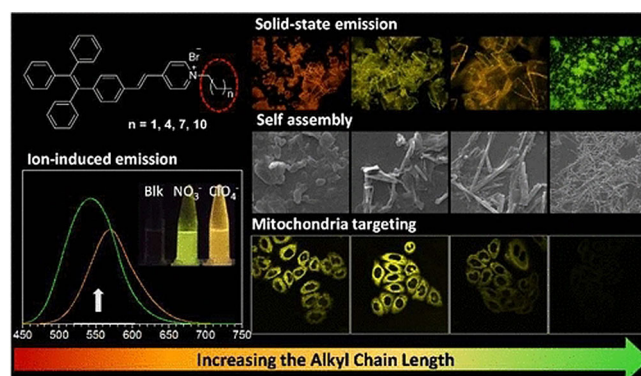


Figure 4. Effect of alkyl chain length on the self-assembly, emission, anion detection, and cell imaging of TPEPy- n ($n = 1, 4, 7, 10$).^[13]

response toward them. Furthermore, the alkyl chain length also affected the cellular uptake selectivity. The longer alkyl chains enabled the fluorogens to penetrate the cell membrane and accumulate in the mitochondria with high specificity.

Attaching amphiphilic groups to AIEgens

Many amphiphiles display strong self-assembly abilities. Introduction of an amphiphile as a whole to the AIE moiety will immediately imbue the AIE portion into a self-assembled structure. For example, Li et al. reported that, after covalently linking bile acids to a TPE core, the bulky amphiphilic bile acid groups directed the self-assembly of the TPE moiety, which led to the formation of well-defined fluorescent vesicles (Figure 5a–d), in which the two bile acids adhered face to face (Figure 5e) to form a hydrophobic pocket.^[14] The formation of these vesicles is driven by multiple intermolecular interactions, such as π - π stacking, hydrogen bonding, and hydrophobic effect. Because there are both hydrophilic and hydrophobic domains in these vesicles, hydrophobic Nile red (NR) and hydrophilic rhodamine B (RB) can be doped simultaneously into the vesicle membrane to generate a noncovalent artificial FRET system. Figure 5f, g shows the fluorescence spectra of the system upon successive addition of NR and RB guest molecules, respectively. The fluorescence intensity of the vesicles at $\lambda = 462 \text{ nm}$ decreased gradually, and a new emission band appeared at longer wavelengths.

Design of amphiphilic polymers

Amphiphilic polymers undergo self-assembly easily. Because AIEgens are often a bulky hydrophobic section composed of many aromatic rings, the idea of designing macromolecules that contained AIE groups arose. To date, the polymer domain has developed many synthesis pathways to obtain amphiphilic polymers with AIE moieties, such as covalent conjugation,^[15] ring-opening reactions,^[16] Schiff base condensation,^[17] free radical polymerization,^[18] reversible addition-fragmentation chain transfer polymerization (RAFT),^[19] and emulsion polymerization.^[20] Some molecular designs may use more than one of these methods.^[21]

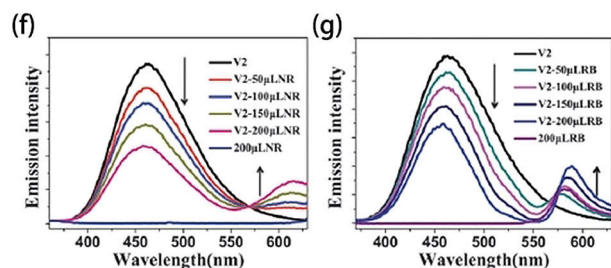
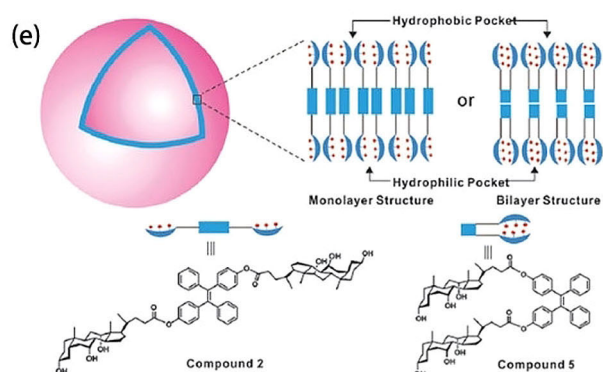
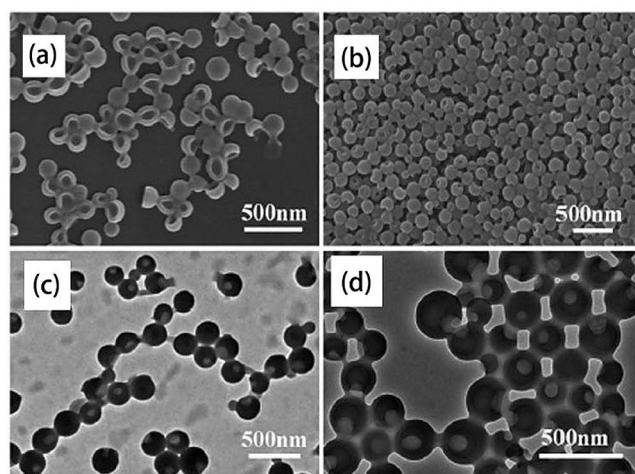


Figure 5. SEM images of the vesicles derived from a) compound **2** at fw = 40% and b) compound **5** at fw = 50% in a water/acetone cosolvent system. TEM images of the vesicles derived from c) compound **2** and d) compound **5**. e) Schematic illustration of the vesicles derived from TPE-bile acid conjugates. FRET effect of the encapsulation of f) NR and g) RB, $\lambda_{\text{ex}} = 325 \text{ nm}$.^[14]

Figure 6a is an example of the introduction of AIEgens into an amphiphilic block copolymer through RAFT polymerization.^[19b] A crosslinkable AIE dye (R-E) with two vinyl end groups was copolymerized with the amphiphilic monomer PEGMA. The resultant copolymer showed typical amphiphilic properties. When dispersed in aqueous solution, it self-assembled into stable nanoparticles (Figure 6c). The core of these particles is composed of aggregated R-E groups, covered by a corona shell of water-soluble PEG blocks.

A similar particle was made by using the ring-opening method. As shown in Figure 7a,^[16c] the AIE monomer PhNH₂ (Figure 7b) with two amino end groups can undergo anhy-

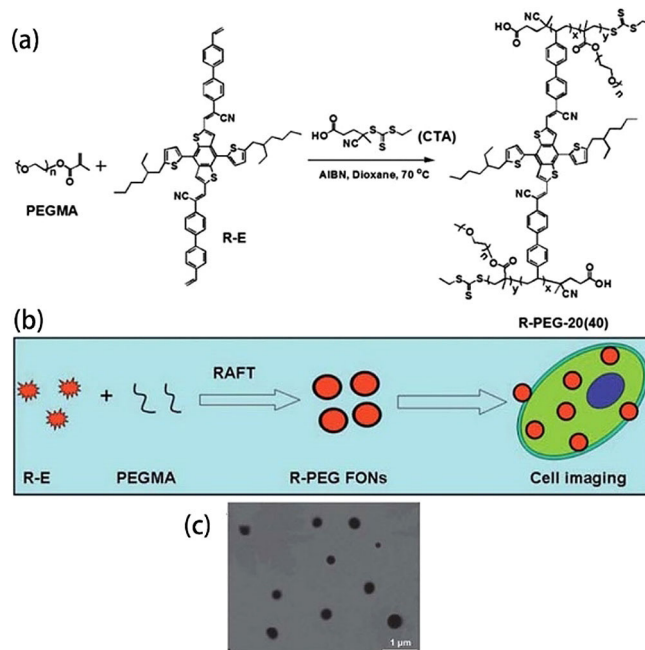


Figure 6. a) Synthetic routes for fabricating R-PEG-20 and R-PEG-40 by a RAFT method with PEGMA and R-E as monomers. b) Schematic of the preparation of R-PEG through RAFT polymerization and its cell imaging application. c) TEM images of self-assembled nanoparticles of R-PEG-20.^[19b]

dride ring-opening polycondensation with 4,4'-oxydiphthalic anhydride (OA). After subsequent cross-linking with polyethyleneimine (PEI), an amphiphilic network polymer (RO-OA-PEI) was obtained, which further self-assembled into stable fluorescent nanoparticles in water (Figure 7a and d). The TEM image shows spherical nanoparticles that range from 50 to 200 nm in diameter (Figure 7c). Because the AIE moieties are covalently linked to amphiphilic molecules, these polymeric nanoparticles display highly desirable stability even under physiological conditions. There are many similar AIE-based polymers, such as TPE-mPEG, synthesized by Liang et al.,^[22] and AIE PCL-b-PEG-based AIE Pdots, reported by Fu et al.^[23] All these particles display strong fluorescence and excellent biocompatibility, which makes them promising for cell imaging^[15, 16b-d, 17-21, 24] and imaging-guided photodynamic cancer therapy applications.^[25]

In addition to making fluorescent particles that can be used for cell imaging, the biomolecule-triggered formation of fluorescent nanoparticles (FNPs) can be an approach to detect special biomolecules. For example, an AIEgen based on phenyl borate may form FNPs with glucose,^[17b] which is accompanied by a drastic enhancement in fluorescence. This considerable glucose-triggered fluorescence switch-on effect makes it a potent detector for abnormal, disease-related levels of glucose (Figure 8).

Molecular design to promote intermolecular hydrogen bonding

Hydrogen bonds in organisms play a very important role in maintaining the structure of biological macromolecules. By

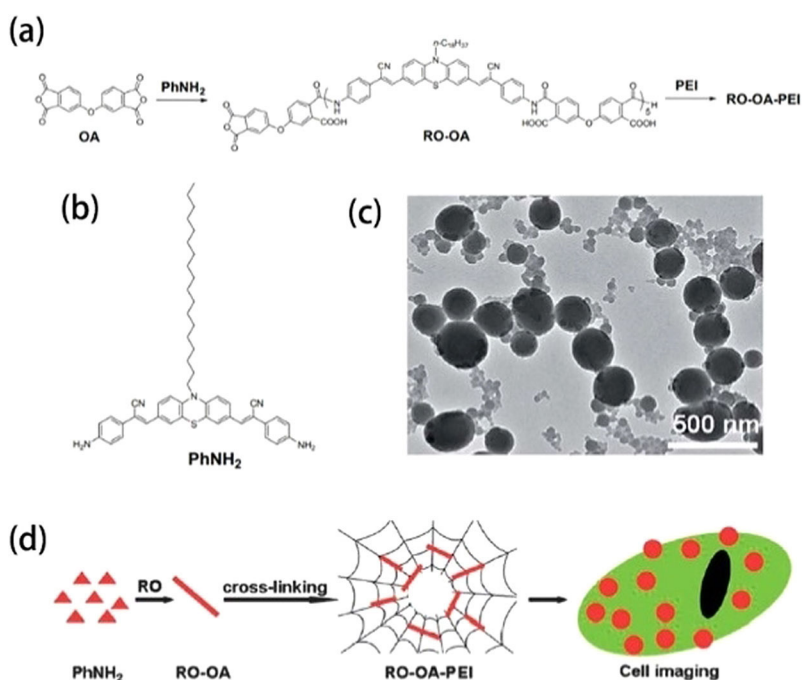


Figure 7. a) Synthesis of RO-OA-PEI. b) Chemical structure of PhNH₂. c) TEM image of FPNs. d) Schematic of the preparation of RO-OA-PEI through anhydride ring-opening polycondensation, and its use in cell imaging.^[16c]

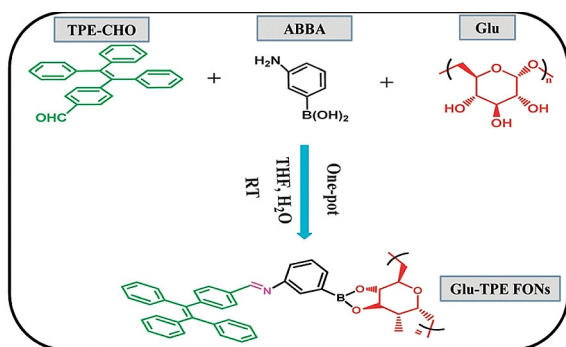


Figure 8. Schematic of the synthesis of Glu-TPE FONs in a one-pot reaction.^[17b]

connecting AIE molecules with molecules that provide hydrogen bonds, different self-assembled structures, such as nanofibers and microloops,^[26] can be formed and thus promote the luminescence of AIE molecules.

Attaching peptide segments to AIE moieties

Peptides show a strong self-assembly ability owing to the formation of inter- or intramolecular hydrogen bonds. AIEgens with a peptide sequence show satisfactory self-assembly ability.^[23b] For example, the peptide sequence GFFY capped with an aromatic group is able to self-assemble into nanofibers.^[27] If the TPE group is used as the aromatic capping group, the resulting TPE-GFFY self-assembles into strongly luminescent fibers. Molecular modeling revealed that the TPE groups are piled up in ordered manner. This packing arrangement restricts the intramolecular rotation of phenyl rings more effectively

and thus results in strong emission (Figure 9a). After attachment of a second peptide sequence of DVEDEE-Ac (Figure 9b), the hydrophilic part becomes dominant and the fluorescent fibers disassemble. However, the strong fluorescence may reappear in the presence of the enzyme caspase-3, which cleaves the link between GFFY and DVEDEE-Ac; thus it is a smart probe to report the level of caspase-3 in cells.

The enzyme cleavage strategy can be generalized to design sensors for a broad spectrum of enzymes. For example, if the peptide sequence is designed to be the substrate of furin, the cleaved product can further self-assemble into fluorescent nanoparticles that can be used to detect the level of furin.^[28]

The peptide sequence does not necessarily need to be very complicated to direct the self-assembly of AIEgens. Besenius et al. reported that the simple phenylalanine-histidine peptide sequence (FHFHF) is able to induce the self-assembly of the AIE luminophore 4,5-bis(phenylthio)phthalonitrile (BPTP) into rod-like micelles in phosphate-buffered saline (Figure 10).^[29] Due to the hydrophobicity of BPTP, it was encapsulated in the core of the micelle, whereas the FHFHF sequence folded into β -sheets on the surface of the hydrophobic rod, which was further attached to C-terminal hydrophilic polycationic dendrons to form a charged cover on the micelle surface (Figure 10a). These anisotropic assemblies are highly stable in serum.

Self-assembly of AIE molecules by covalently linking amino acids to AIEgens

Compared with designed peptide sequences, individual amino acids covalently linked to some AIEgens were found to be sufficient to facilitate the self-assembly of AIEgens.

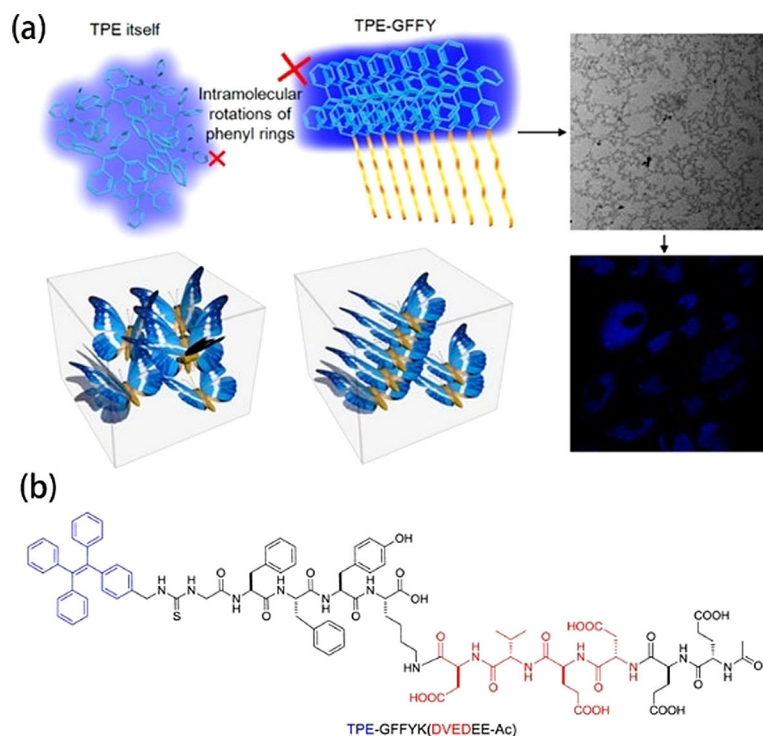


Figure 9. a) Schematic comparison of the more ordered TPE-GFFY aggregates versus TPE only. TPE-GFFY can self-assemble into filamentous network nanostructures and emits blue light under CLSM. b) Chemical structure of TPE-GFFYK(DVEDEE-Ac).^[27]

Tang et al. reported that the TPE moiety can be combined with L-valine or L-leucine,^[30] and the resultant molecules can self-assemble into helical nanofibers in a cast film (Figure 11). Amazingly, these fibers exhibit aggregation-induced circular dichroism (AICD) and circularly polarized luminescence (CPL), which indicates that the chirality is transferred from the amino acid to the TPE moiety. Similar results can be obtained for TPE with two valine-containing attachments (TPE-DVAL),^[8] but the helical ribbons are more uniform in size (Figure 12).

These AIEgens modified with amino acids are very promising for the fabrication of efficient CPL devices for biosensing and optoelectronic applications. It is noted that if the amino acid groups are replaced with sugar moieties, similar chiral helices can be obtained.^[31] A good example is the silole derivative with a chiral sugar head. It self-assembles into right-handed helical nanoribbons that preserve the AIE properties and emit right-handed circularly polarized luminescence.^[31]

Molecular design with van der Waals forces

Van der Waals forces exist universally between molecules and atoms. Application of the additive property of van der Waals forces allows us to generate strong intermolecular interactions simply by increasing the molecular weight. With this principle, the self-assembly of AIEgens can be enhanced by judicious covalent modification.

A single TPE core can hardly form well-defined structures in solution, but two TPE units coupled into one molecule may

give well-defined microfibers when crystallized from the solvent.^[32] These crystalline microfibers display a extremely high fluorescence quantum yield and can be made into luminescent films (Figure 13). Furthermore, covalent linkage of a benzene ring to each of the propellers in opposite positions (DPBPPE in Figure 13) can result in the formation of well-defined self-assembled structures, but these structures are not as good as those formed by BTPE, and the fluorescent quantum yield is also lower than the BTPE fibers.

This significant enhancement in van der Waals forces, triggered by large molecular weight, can be generalized for a number of systems. Xu et al. found that when the TPE group is linked to a polyhedral oligomeric silsesquioxanes group (POSS) by a flexible spacer, the resultant POSS-ANs were able to aggregate into nanoparticles and emit strong fluorescence.^[33] Tang et al. showed that biphenyl-based triazoles can also be used as a spacer for nanofiber formation.^[34] It should be noted that as the van der Waals forces bring the molecules together, other possible interactions may also occur between the self-assembled molecules. For example, π - π stacking may occur between benzene rings in the BTPE system, and the hydrophobic effect of the alkyl chains may contribute to the self-assembly of AIEgens with alkyl spacer chains.

π - π stacking

Under normal conditions, π - π stacking will cause excimer and exciplex formation, which leads to nonradiative channel consumption and thus weakens the emission intensity. However, Marin et al. found that if the distance between fluorophoric units is longer than the π - π stacking distance, the formation of excimers and exciplexes will be hindered, which leads to an increase in emission intensity.^[35] They designed a new AIE molecule based on triazoles, phenothiazine, and pyridine-*N*-oxide units. Because of the immiscibility of triazoles in water, a large fraction of water will force fast segregation, and thus does not allow close packing. This is the main reason for the significant increase in luminescence in the crystalline state.

Similarly, if π - π stacking does not occur between AIE groups, it will not cause fluorescence quenching. Bhosale et al. synthesized two π -conjugated porphyrin molecules with tetraphenylethene (Figure 14a).^[36] This compound is able to self-assemble in both nonpolar and polar solvents. In particular, it forms ring-like nanostructures in polar organic solvents (Figure 14b). The main driving force for self-assembly is the extensive π - π interactions between the TPE and the thiophene moiety. Each phenyl ring of TPE has face-to-edge interactions with two other rings and each thiophene unit exhibits face-to-face stacking with two other thiophene units in other layers. Similar AIE self-assembled structures with π - π interactions as the driving force have been published by Bhosale et al.,^[37] Tian et al.,^[38] and Tang et al.^[39]

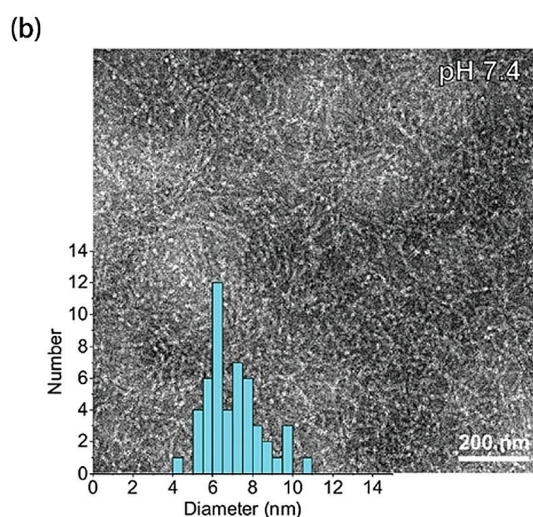
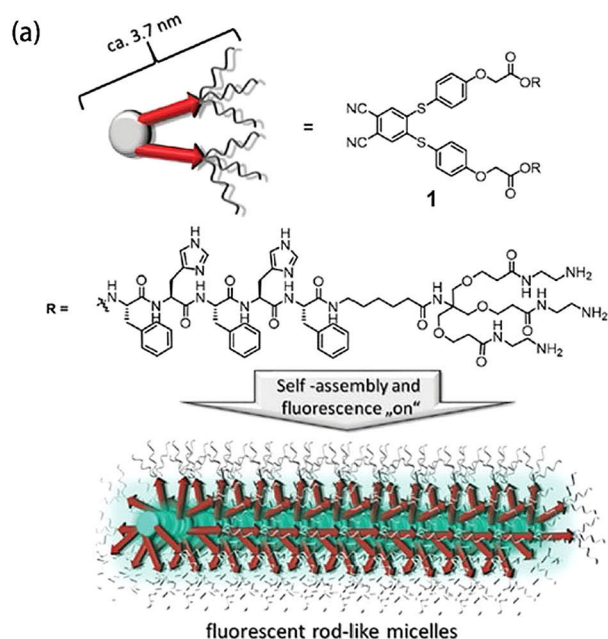


Figure 10. a) Schematic representation of the self-assembly of cationic peptide amphiphiles into luminescent rodlike micelles. b) TEM image of the rodlike micelles.^[28]

Linear donor–acceptor (DA) structures in AIEgens

A molecule with both electron donor (D) and acceptor (A) groups has a large dipole moment, and is able to self-assemble through dipole–dipole interactions. Tian et al. reported the DA-type AIE molecule ED (see Figure 15) by changing the oxygen atom for an electron-rich *N*-ethyl group in a quinolinemalononitrile-based molecule (BD). The DA effect results in a highly twisted conformation for ED, which avoids π – π stacking of the quinolinemalononitrile moiety. Driven by dipole interactions, the ED molecules self-assemble into extremely long intensive red-emitting wave guiding fibers.^[40]

Han et al. systematically studied the self-assembly of AIE-active Schiff base compounds.^[41] Theoretical calculations suggested that the DA groups take antiparallel conformation when stacking (Figure 16), which indicates that the electrostatic

effect plays an important role in the self-assembly of DA-type AIE molecules.

The electronic structure of DA molecules can be influenced by substituent groups, which impact the degree of π conjugation in the molecule. Therefore, the substitution of DA molecules has a considerable effect on the self-assembled structure and emission colors. Ouyang et al. synthesized four electron-donor-substituted AIE compounds, BSPD-OMe, BSPD, BSPD-Me, and BSPD-OH, which can self-assemble into four different morphologies (microblocks, microparticles, microrods, and nanowires)^[42] with three emission colors (green, yellow, and orange; Figure 16). This result shows that different substituents are important in the self-assembly of DA-type AIE molecules, and offer a good method to control the structure and property of AIE materials. Stronger electron-donor substituents (OMe and OH) can twist the molecular conformation, decrease the degree of π conjugation, increase the energy gap, and induce morphology variation and a blueshift in the emission colors. Similar research is conducted by Tang et al.,^[43] Yang et al.,^[44] Šket et al.,^[45] Tian et al.,^[46] and Wang et al.^[47]

Self-assembly of AIE molecules through non-covalent interactions

Supramolecular interactions are an alternative strategy to construct new building blocks that are able to self-assemble.^[48] Compared with the use of covalent bonds to create desired functional structures, the supramolecular protocol that connects the desired moieties through noncovalent interactions has many advantages,^[48b] such as facile preparation, high yield, judicious choice of functional units, responsiveness to external stimuli, and inherent error correction.^[49] These merits endow supramolecular AIEgens with the promising ability to construct advanced functional materials.^[48a] There are some reviews on the manipulation of AIE with supramolecular macrocycles.^[50] Here, we summarize the literature on supramolecular AIE structures according to different noncovalent interactions.

Electrostatic interactions

Electrostatic interactions are universal in nature, and occur between any combination of oppositely charged molecules or a pair of molecules that act as electron donors and acceptors. A stable complex can form in the charge-balanced state, which is a supramolecular unit capable of self-assembly into hierarchical structures. Here, we show some examples of self-assembled AIEgens with different electrostatic interactions.

Ionic interactions

Organic molecules with opposite elementary charges are able to form ion-pair complexes. Compared to the individual molecules, the neutral ion-pair complex has a greater hydrophobic effect and displays stronger self-assembly ability.^[51] It is known that ionic self-assembly (ISA) is a facile and efficient approach to construct novel functional materials by binding oppositely charged building blocks together through electrostatic interac-

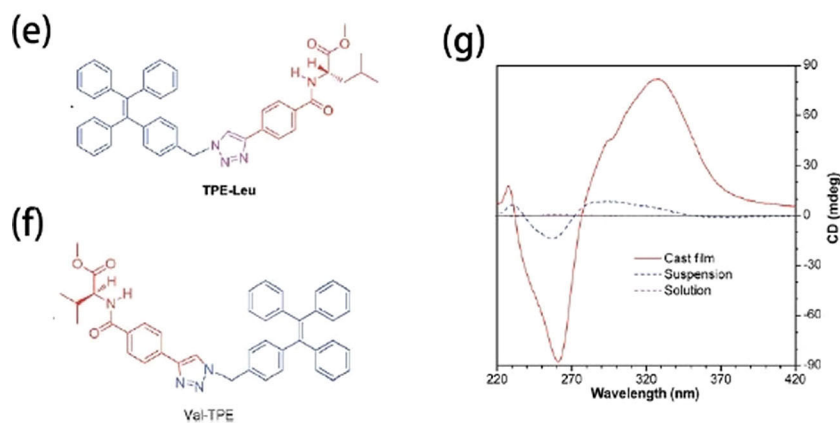
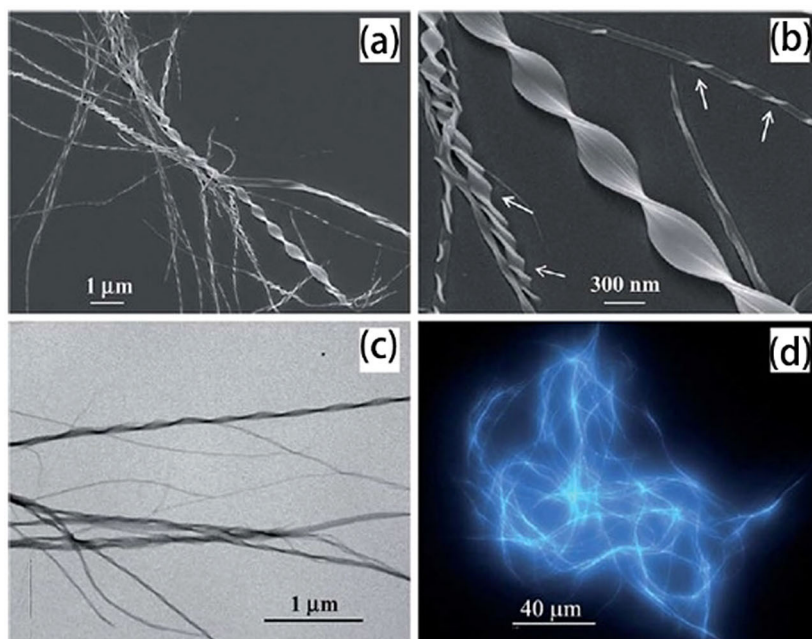


Figure 11. a, b) SEM, c) TEM, and d) fluorescence microscopy images of the aggregates of TPE-Leu formed in DCE/hexane (1:9 v/v), concentration: 10–14 μ M. Molecular structures of e) TPE-Leu and f) Val-TPE. g) CD spectra of TPE-Leu in DCE and DCE/hexane (1:9 v/v) suspension (concentration 10–4 μ M) and as a cast film prepared by natural evaporation of its solution in DCE (0.66 mg mL^{-1}).^[30]

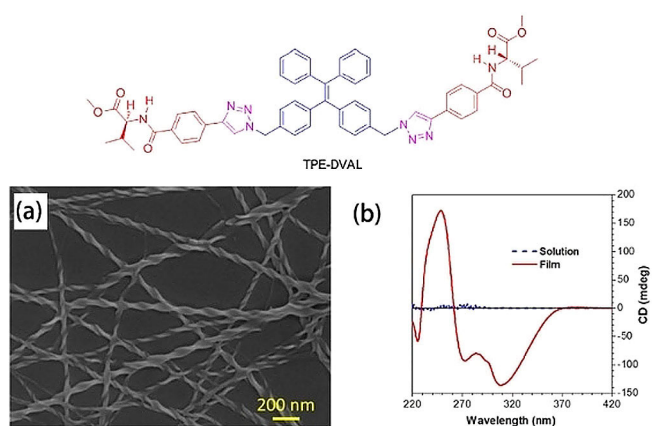


Figure 12. Evaporation-induced helical ribbon self-assembly of TPE-DPAL, which displays enhanced CPL behavior when self-assembly occurs in the microfluid channels.^[8]

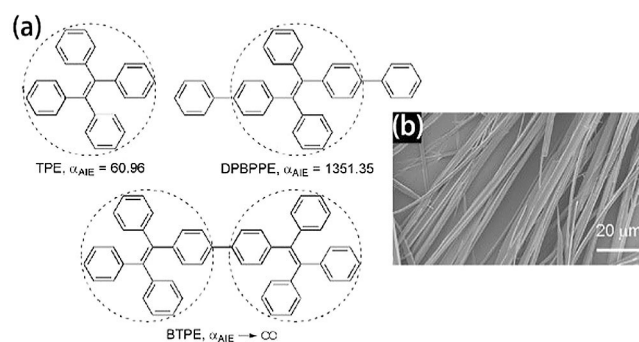


Figure 13. a) The structures of TPE, DPBPPE, and BTPE. b) SEM image of BTPE microfibrils.^[32]

tions.^[52] This principle can be used to direct the self-assembly of ionic AIEgens. For example, Yan et al. neutralized the charg-

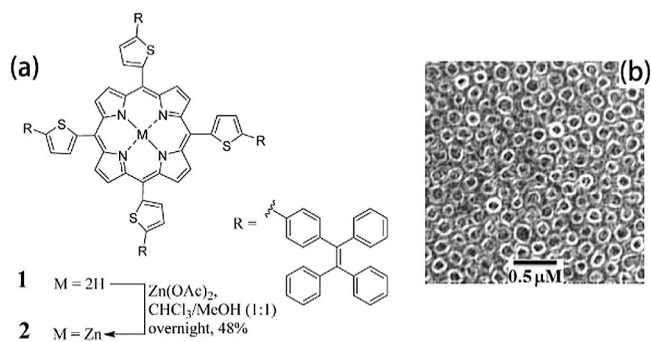


Figure 14. a) Molecular structure of TPE-porphyrins. b) TEM images of TPE-porphyrins in CH₃CN/MeOH.^[36]

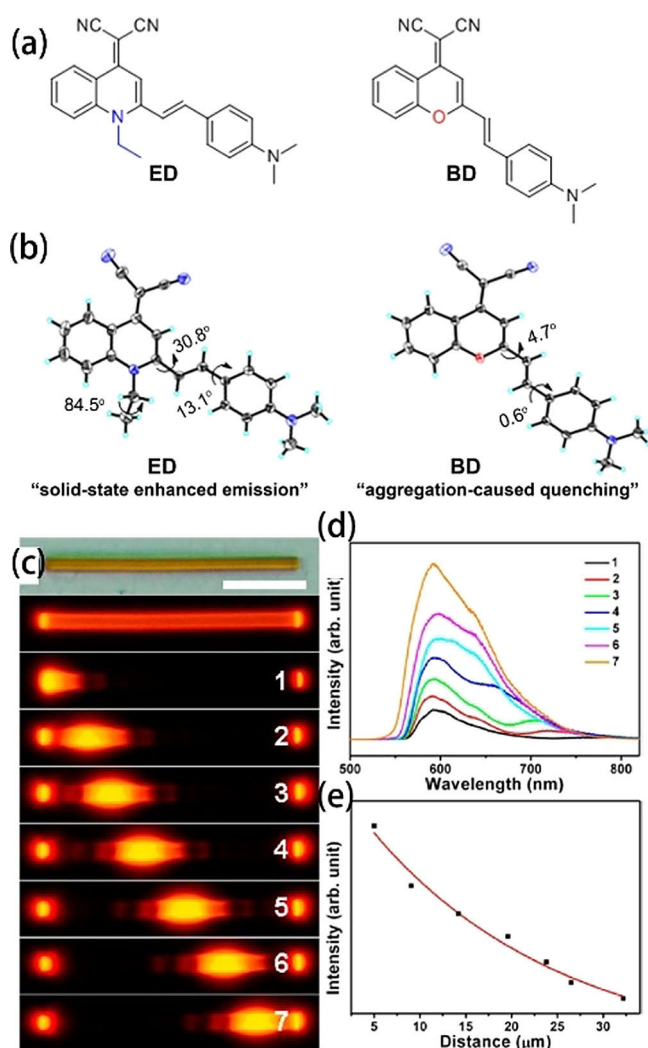


Figure 15. a, b) The molecular structures of ED and BD; c, e) the wave-guiding property of the red-emissive fiber.^[40]

es of a coordinating AIEgen TPE-BPA with a surfactant,^[53] which resulted in the formation of a pseudo-nonionic supramolecule (Figure 17). The alkyl chain of the surfactant fits in the voids between the TPE rotators. The resultant supramolecular unit can self-assemble into vesicles through the hydropho-

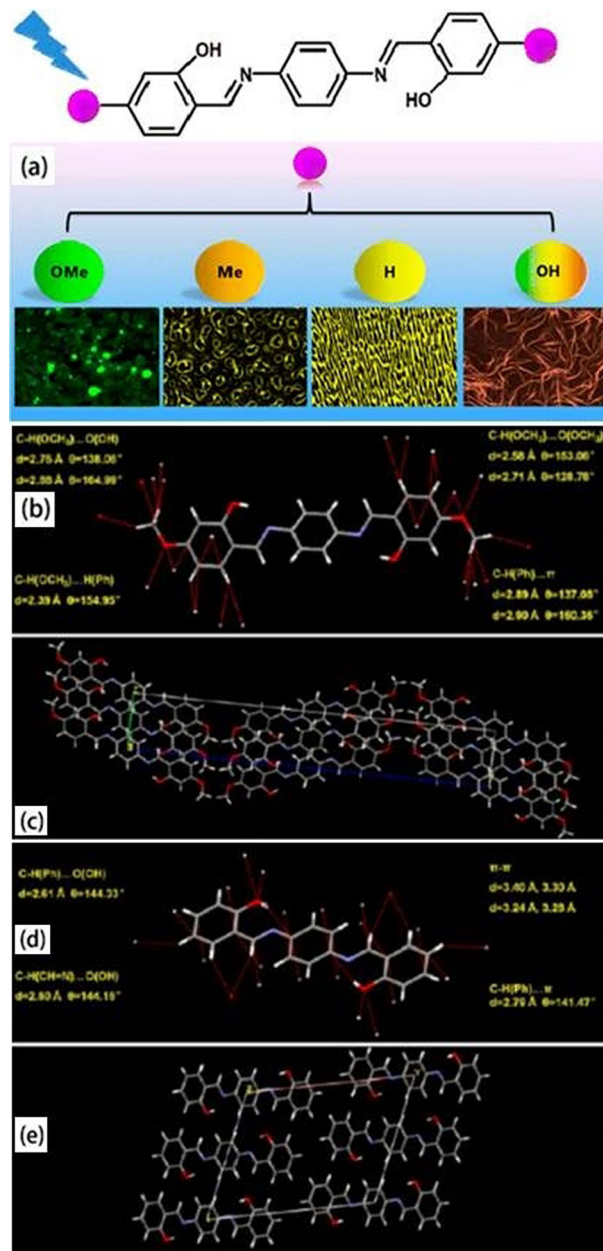


Figure 16. a) Self-assembled structures impacted by different substituent groups.^[42] b) Single-crystal structure and intermolecular forces of BSPD-OMe. c) Packing in the BSPD-OMe single crystal. d) Single-crystal structure and intermolecular forces for BSPD. e) Packing in the BSPD single crystal.

bic effect. After silication, this vesicle can be coated a layer of SiO₂, which retains the fluorescence, and grafted folic acid can target this vesicle to cancer cells. In this way, a fluorescent drug carrier capable of self-guiding and self-imaging is created, which makes it possible to track the entire drug delivery pathway in situ.

The fluorescence of the vesicles is closely related to the intactness of the vesicle membrane. If the vesicle membrane becomes looser or disassembles, the fluorescence becomes weaker.^[54] This effect can be used to construct enzyme-responsive fluorescence vesicles. If the surfactant CTAB is replaced by the substrate of cholinesterase myristoylcholine chloride

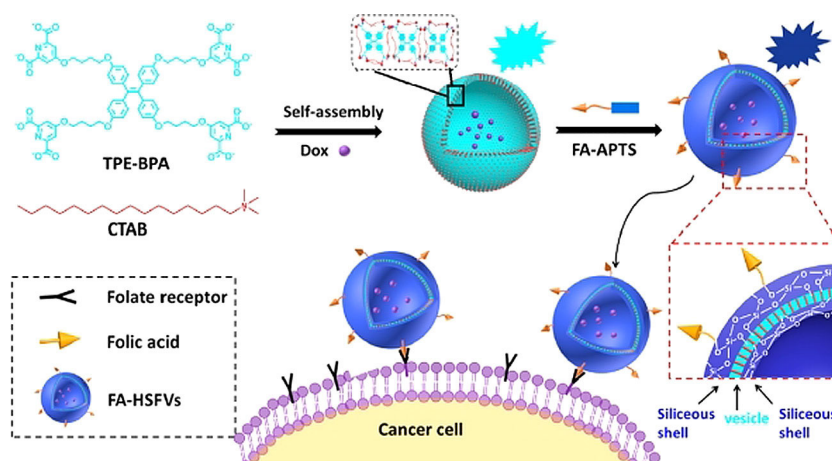


Figure 17. Illustration of self-assembly of folic acid-modified silicate fluorescent supramolecular vesicles (FA-HSFVs) and their use in cancer-cell targeting.^[53]

(MChCl), the ionic interaction between TPE-BPA and MChCl can form a supra-amphiphile, TPE-BPA@8MChCl (Figure 18), which then self-assembled into vesicles.^[55] This vesicle may spontaneously target regions with high levels of acetyl or butyl cholinesterase (AChE). These enzymes can cleave the MChCl molecule and disassemble the vesicles. This is accompanied by a reduction in fluorescence and release of the entrapped enzyme inhibitor drugs. As a result, the abnormally high enzyme level can be reduced, which is expected to have potential applications in the treatment of Alzheimers' disease.

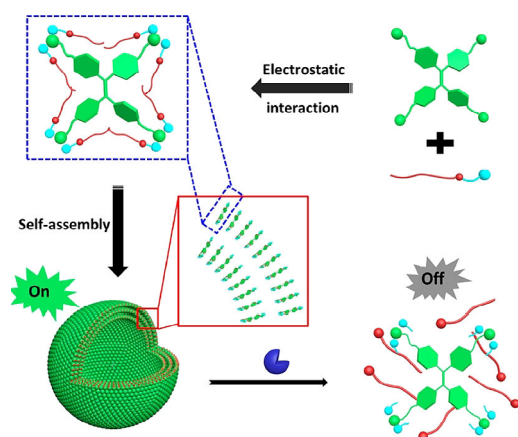


Figure 18. Illustration of the self-assembly and disassembly process of fluorescent vesicles, caused by the enzyme AChE.^[55]

A double-chained surfactant may induce more complicated self-assembled AIEgen structures. Ren et al. designed an AIE-active ionic supramolecule TPE-DOAB (Figure 19a). At room temperature, this complex can self-assemble into a liquid crystal (LC) phase composed of low-ordered helical columns. On heating, it enters another LC phase with highly ordered helical molecular stacking, which is induced by variation in the degree of peripheral chain motion. Figure 19b shows the molecular stacking mode of TPE-DOAB in a helical column. Owing to efficient aggregation, a quantum yield as high as 46% can

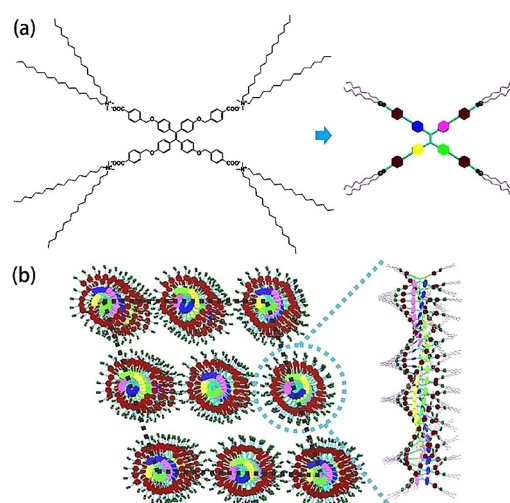


Figure 19. a) Schematic diagram of the TPE-DOAB structure. b) Model of the helical column in the monoclinic lattice ($P2_1$) of TPE-DOAB.^[56]

be achieved in the solid state. Similar AIE-based LC research work can be found in Ref. [56].

Charge transfer interaction

Ionic interactions are strong electrostatic interactions, whereas in many cases there may be a much weaker electrostatic effect between molecules. For example, if two individual molecules are electron-rich and electron-deficient, respectively, they are able to form a complex through a charge-transfer (CT) effect. Zhang et al. reported an experimental procedure to construct supramorphiles through a CT interaction.^[57] In the AIE research community, Huang et al.^[58] used electron-rich naphthalene (TPE-NP) and electron-deficient paraquat (TPE-PQ) as a CT pair, both are covalently linked to the TPE core. The formation of a CT complex results in a robust building block that can self-assemble further into 1D nanorods in water (Figure 20a–b). Because the TPE-PQ molecule can form a much more stable inclusion complex with the negatively charged water-soluble pil-

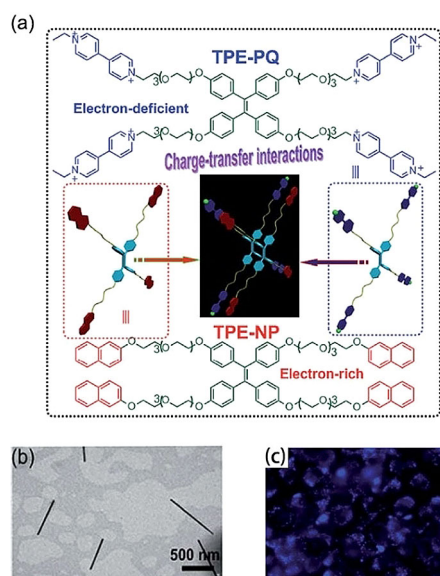


Figure 20. a) Illustration of the CT interaction between TPE-PQ and TPE-NP. b) TEM image of the self-assembled structure of the CT complex. c) Confocal images of live MCF-7 breast cancer cells after incubation with H₄⊃TPE-PQ@TPE-NP (H, TPE-PQ, and TPE-NP concentrations: 1.00×10^{-4} , 2.50×10^{-5} , and 2.50×10^{-5} M, respectively).^[58]

lar[6]arene (H4), addition of H4 to the nanorod suspension results in disassembly of the TPE-NP/TPE-PQ CT complex and, consequently, the nanorods. This causes a drastic reduction in the fluorescence. However, in an acidic environment, the H4 molecules are positively charged. This co-charge produces repulsion with TPE-PQ, which results in disassembly of the H4⊃TPE-PQ inclusion complex and leads to fluorescence recovery. Therefore, when a system composed of H4/TPE-NP/TPE-PQ is added to tumor tissue, in which the pH is lower than normal, the AIE-active CT complex is formed and can be used for cancer-cell imaging (Figure 20c).

Coordination interactions

Coordination links have proved to be very powerful in the construction of supramolecular structures.^[59] This is because the energy for a coordination bond is close to that of a covalent one, which makes the coordinated structures very stable. In addition, the geometrical constraints of a coordination field may regulate the orientation of ligand molecules in space, which makes coordination interactions very attractive for the construction of supramolecular structures with fascinating topologies.^[60] When coordination interactions encounter multi-armed AIEgens, the topological organometallic system becomes highly fluorescent because the intramolecular rotation of the arms is restricted by the framework.

Microcycles formed by metal-coordination-mediated linking of coordinating AIEgens

The multiarm nature of TPEgens allows multiple coordinating sites to be generated within one molecule. This is beneficial

for the creation of coordination supramolecules.^[61] The simplest example of coordination supramolecule formation is the bisligand-type AIEgen linked through coordination interactions. Yang et al.^[62] designed and synthesized a series of crease line shape bisligands by covalently attaching the 2,2':6',2''-terpyridine (TPY) coordinating group to the neighboring two arms of TPE (Figure 21a–c). On coordination with Cd^{II}, the TPE-TPY bisligand can be connected into rosette-like macrocycles. Detailed results can be seen in Figure 21h–s, with AFM and SEM images and proposed 3D stacking structures. If two extra TPY ligands are attached to the remaining two arms and the arms are extended by one or two benzene units, 2nd and 3rd generation macrocycles can be created, respectively (Figure 21d). As shown in Figures 21d–f, as the water ratio in the solvent is increased, the color of the macrocycle solution gradually becomes yellower. Dynamic light scattering (DLS) shows that, in acetonitrile/water mixtures, metallosupramolecules further aggregate into nanospherical particles (Figure 21g). The size, shape, and composition of these metallosupramolecules can be precisely controlled, and they may have broad applications in, for example, light-emitting diodes, sensors, photoelectric devices, bioimaging.

It is known that imine groups, such as Schiff bases and hydrazones, have a strong tendency to bind copper ions. Zheng et al.^[63] and Hu et al.^[64] designed and synthesized three types of Schiff base molecule (Figure 22a–c). All these molecules can self-assemble into well-defined structures in mixed solvents (Figure 22d–f). The emission of these self-assembled structures can be severely quenched by Cu²⁺. In contrast, the fluorescence intensity did not change notably on addition of other metal ions. This makes the Schiff base molecule a sensitive probe for Cu²⁺ (Figure 22g). A microscopy study revealed that Cu²⁺ induces a barrel-like structure of AIE b) or AIE c). Cu²⁺ was tightly held in the cavity of the barrel through coordination bonds. This Cu²⁺ capturing behavior is very similar to the CopC protein (Figure 22h).

Coordinating fluorescent macrocycles based on multiple Lego blocks

The oriented nature of coordinating interactions allows us to connect different multitopic ligands into well-defined topological structures. The AIEgens can be used as one of the ligands. Stang et al.^[49,59a,65] designed a series of metal acceptors and organic donors. The coordination between the metal acceptor and different donors can lead to diverse macrocycles. For example, metal acceptor **6** ([Pt(PEt₃)₂(OSO₂CF₃)₂]) and two organic donors **3,4** or **3,5** may self-assemble into tetragonal prismatic metallocages **1** and **2** (Figure 23a).^[65b] The polarity of the solvent has a large effect on aggregation, and thus the electronic state, of the metallocages, which leads to different emission colors^[65b] (Figure 23b–d). The coordination interaction increases the MLCT process in the metal cages, whereas the AIE moiety displays conformation-dependent emission. The combination of these two effects makes the emission of the metallocages very sensitive to the solvent environment. For example, the emission color can be influenced by structurally similar

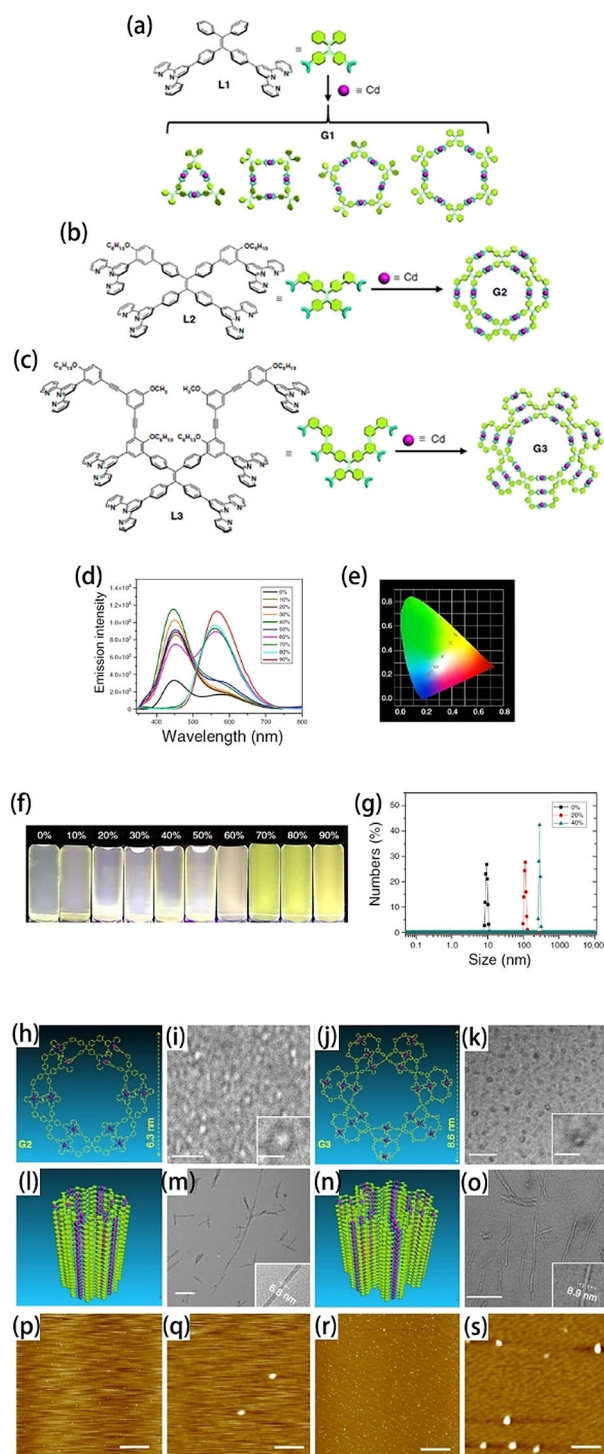


Figure 21. a)–c) Self-assembly of supramolecular rosettes G1–G3. d) Fluorescence spectra ($\lambda_{\text{exc}} = 320 \text{ nm}$, $c = 1.0 \mu\text{M}$), e) CIE 1931 chromaticity diagram, f) photographs of G2 in $\text{CH}_3\text{CN}/\text{water}$ at various water fractions, and g) DLS of G2 in $\text{CH}_3\text{CN}/\text{water}$ mixtures. h, j) Representative energy-minimized structure, i, k) TEM images, l, n) proposed 3D stacking structure, m, o) TEM images of nanotubes, p–s) AFM images with scale bar of $2 \mu\text{m}$ and 100 nm of G2 and G3, respectively.^[62]

ester compounds. A slight variation in the structure of the esters may trigger significant wavelength shifts in the visible region (Figure 23e).

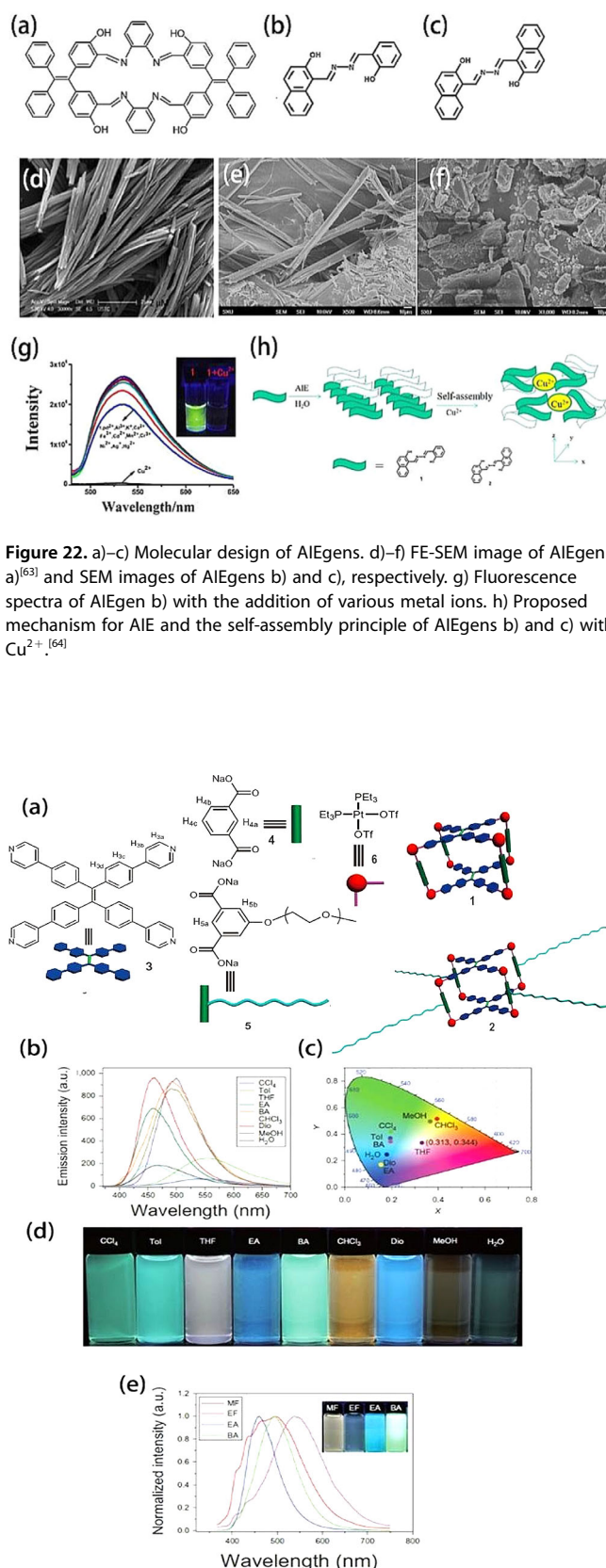


Figure 22. a)–c) Molecular design of AIEgens. d)–f) FE-SEM image of AIEgen a)^[63] and SEM images of AIEgens b) and c), respectively. g) Fluorescence spectra of AIEgen b) with the addition of various metal ions. h) Proposed mechanism for AIE and the self-assembly principle of AIEgens b) and c) with Cu^{2+} .^[64]

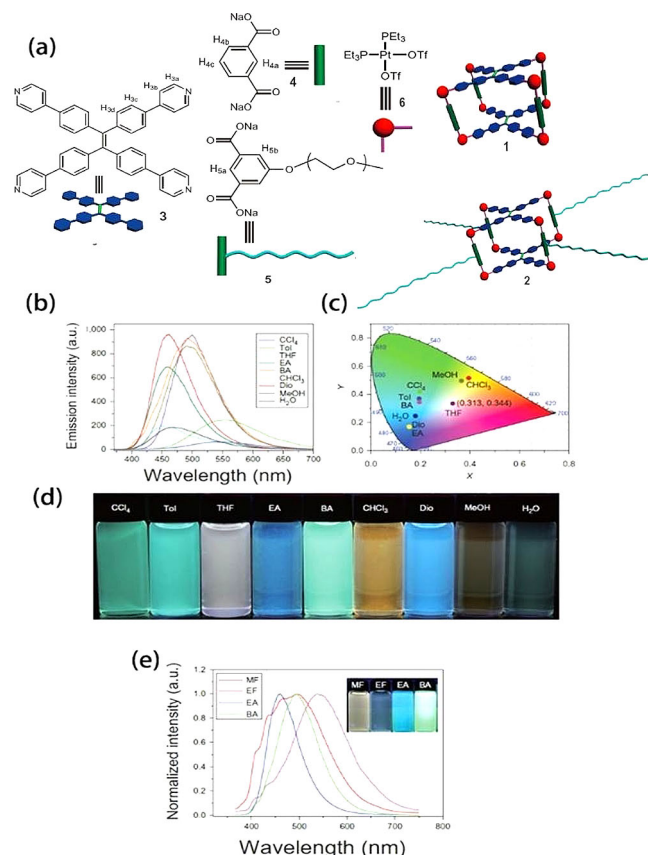


Figure 23. a) Synthesis of tetragonal prisms **1** ($3 + 4 + 6$) and **2** ($3 + 5 + 6$). b) Fluorescence emission spectra, c) CIE chromaticity coordinates, and d) photographs of metallacages **2** in different solvents. e) Normalized fluorescence emission spectra and inset: photograph of **2** in different ester solvents.^[65b]

PEG chains on the tetragonal core influence the aggregation of **2** in mixtures. As the water fraction is increased, metallocage **1** self-assembles into irregular nanoparticles, regular nanospheres, and net-like aggregates. However, the morphology of the aggregates formed by metallocages **2** only change from irregular nanoparticles to regular nanospheres.

The Lego strategy can be generalized to diversified blocks. As shown in Figure 24a,^[65c] a metallarhomboid and a triangle

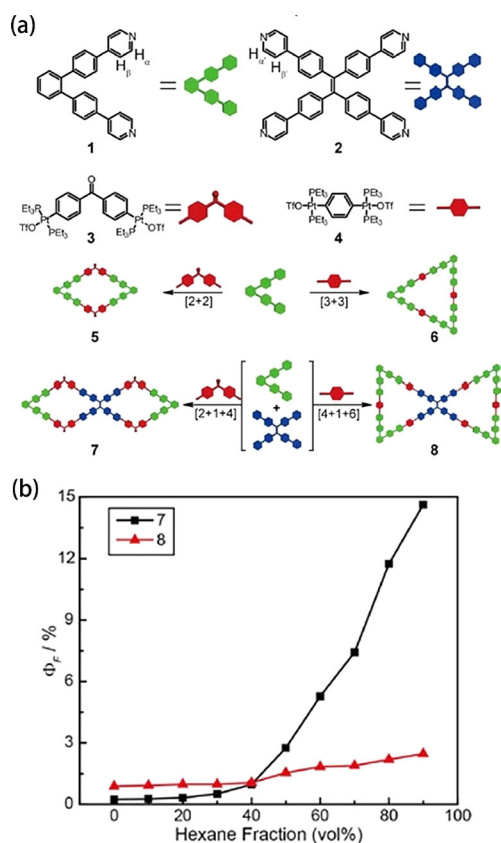


Figure 24. a) Syntheses of double rhomboid **7** and double triangle **8** by multicomponent coordination-driven self-assembly. b) Quantum yields of **7** and **8** in CH_2Cl_2 /hexane with different hexane fractions.^[65c]

were designed by using a TPE-based tetrapyrindyl donor and Pt^{II}-coordinated complexes. Fused rhomboid **7** shows weaker fluorescence in dilute solutions relative to that of fused triangle **8**, whereas a reversal of emission intensities was observed in the aggregated state (Figure 24b). This phenomenon is due to differences in the shapes of the fused polygons. In dilute solution, immobilization of the TPE moiety within a double triangular structure imposes more restrictions on its intramolecular motions than immobilization in a double rhomboidal structure. Conversely, in aggregates the relative flexibility of the rhomboidal skeletons may allow them to aggregate much more tightly than the rigid triangular structures and thus **7** forms larger aggregates than **8**. Furthermore, double triangle **8** contains a higher number of Pt centers than **7**, which may increase the intersystem crossing and thus cause a drop in emission efficiency.

A similar strategy can be used to create pure TPE-based 2D hexagonal metallacycles and 3D drumlike metallocages (Figure 25a–b). Stang et al. achieved this by using TPE-based di-Pt^{II} as the coordinating metal and TPE-based dipyrindine as the bis-ligand. The coordination reaction led to the formation of 2D cycles and 3D cages. The molar absorption coefficients (ϵ), fluorescence emission intensities, and quantum yields (Φ_F) of these metallacycles can be influenced by different counter anions in CH_2Cl_2 , in the order $\text{PF}_6^- > \text{OTf}^- > \text{NO}_3^-$ (Figure 25c–d). All six metallacycles formed well-defined spherical nanoaggregates in CH_2Cl_2 /hexane (Figure 25f–j). Counterions may influence the photophysics of the assemblies, particularly when they influence the solubility of the resulting metallacycles or cages.^[65d]

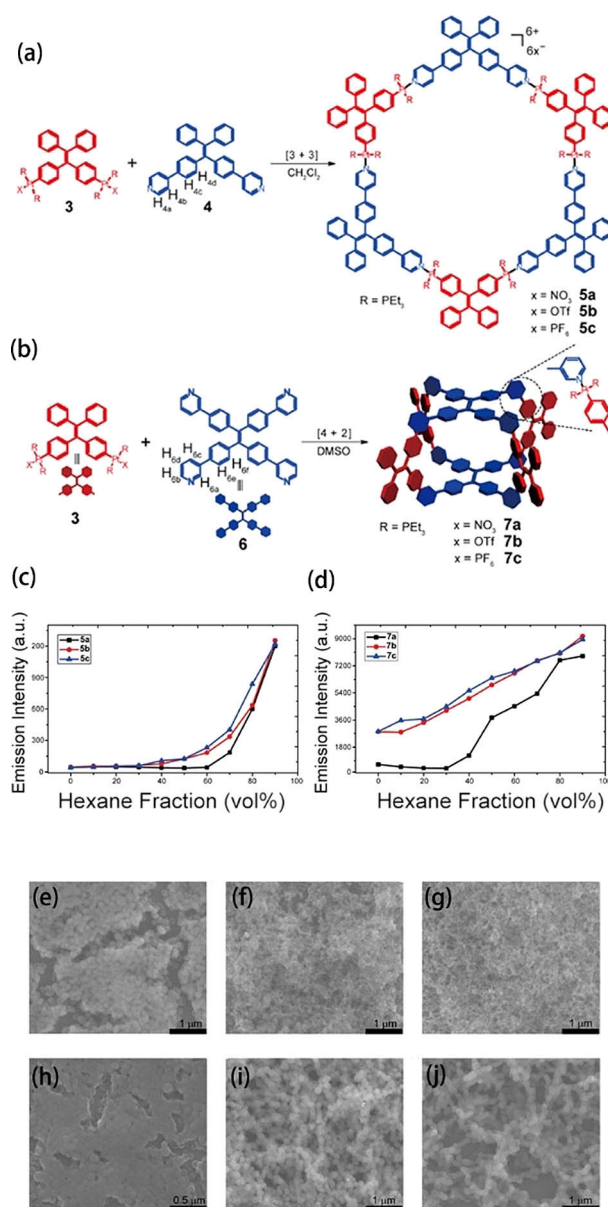


Figure 25. Synthesis of a) metallacycle **5** and b) metallacage **7**. Emission intensity versus hexane fraction with respect to different counterions for c) **5** and d) **7**. SEM images of e) **5a**, f) **5b**, g) **5c**, h) **7a**, i) **7b**, and j) **7c** in CH_2Cl_2 /hexane (90% hexane).^[65d]

TPE-containing metallacages can act as a “turn-on” sensor for amino acids due to the strong binding of some amino acids to metal ions.^[59a] In methanol/water (1:1 v/v), the cage is nearly nonemissive, but when a thiol-containing amino acid (cysteine or glutathione) is added to the solution, it emits strongly. Similar TPE-based discrete organoplatinum(II) 2D metallacycles can be used for sensing nitroaromatics.^[49]

Hierarchical self-assembly of metallogages

The coordination-driven macrocycles based on different Lego blocks can also undergo hierarchical self-assembly, which gives them better functionality. Yang et al. synthesized a positively charged organoplatinum(II) metallacycle with dangling TPE units.^[66] On addition of negatively charged heparin, the formation of a “pearl necklace” structure driven by electrostatic complexation restricted the free motion of the TPE group and resulted in dramatic fluorescence enhancement (Figure 26a–c).

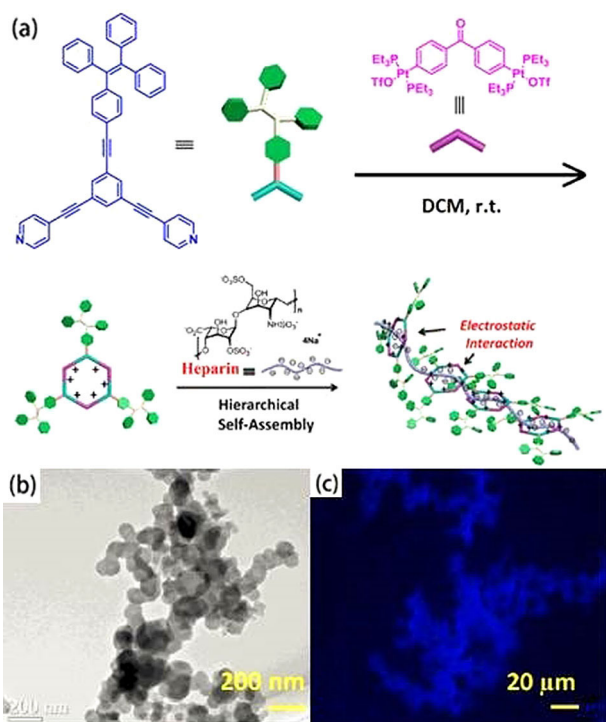


Figure 26. a) Schematic illustration of hierarchical self-assembly through coordination-driven self-assembly and electrostatic interactions. b) TEM image of the pearl-necklace microstructures of the hierarchical self-assembly.^[66] c) CLSM image of the pearl-necklace structure.

This can be used as a “turn-on” probe for heparin detection.

Synthetic chemistry allows the design of various tectons. If crown ether is attached to one of the Lego blocks in the metallacycle, threading further metallacycles into the network becomes possible. Figure 27 is an example of this type.^[65a] A tetragonal prismatic cage with four appended 21-crown-7 (21C7) moieties in its pillar regions was prepared from *cis*-[Pt(PEt₃)₂(OTf)₂], tetraphenylethene (TPE)-based sodium benzoate ligands, and linear dipyriddy ligands (Figure 27a). Further addi-

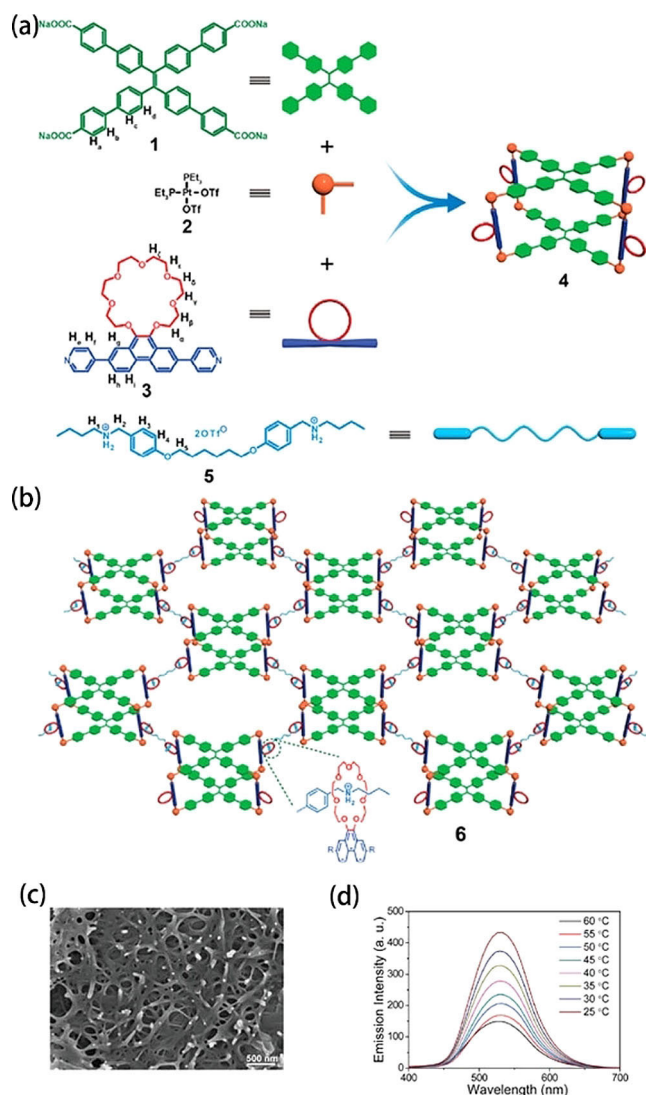


Figure 27. a) Self-assembly of 21C7-functionalized metallacycle **4**. b) Formation of crosslinked **6** from metallacycles **4** and bisammonium salt **5**. c) SEM image of the gel. d) Temperature-dependent fluorescence spectra of the gel.^[65a]

tion of a bisammonium linker crosslinked the cages into a network (Figure 27b–c). On gelation, the fluorescence intensity increased drastically. The fluorescence of the gel decreased on heating and returned to its original state on cooling (Figure 27d). The introduction of metallacycles as the junction not only benefits the supramolecular gel emission properties but also imparts enhanced stiffness and improved self-healing properties to the gel.

The hierarchical self-assembly of AIE-based macrocycles can be a one-pot process when amphiphilic polymers are attached to the Lego blocks. Stang et al. synthesized a four-armed amphiphilic copolymer,^[67] Pt-PAZMB-*b*-POEGMA, with metallacycle **M**, in which the TPE derivative acts as an AIE functional group for live-cell imaging and phenPt is an anticancer drug (Figure 28). Under different experimental conditions, this copolymer can self-assemble into nanoparticles or vesicles to encapsulate anticancer drugs.

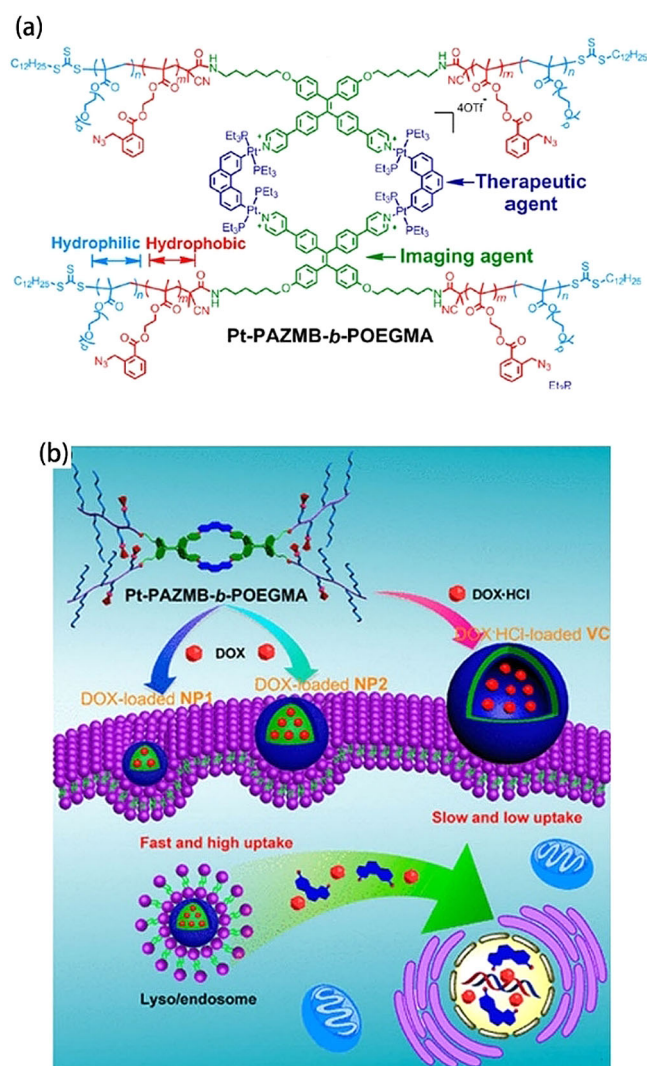


Figure 28. a) Structure of the Pt-PAZMB-*b*-POEGMA block copolymer and b) hierarchical self-assembly of the polymer into vesicles for drug delivery.^[67]

Host-guest interactions

Host-guest chemistry has been widely employed to construct self-assembled supramolecular structures. To date, cyclodextrins (CD), crown ethers, calixarenes, cucurbiturils, pillararenes, cyclotrimeratrylenes, cryptophanes, carcerands, and foldamers are mainly used as hosts to accommodate specific guests.^[7] Here, host-guest interactions that facilitate the self-assembly of AIE molecules is summarized.

Pillararene-based small molecules

Pillar[*n*]arenes, in which repeating units are connected by methylene bridges at the *para*-positions of 2,5-dialkoxybenzene rings (e.g., pillar[5]arenes, pillar[6]arenes, and other high-level pillar[*n*]arenes ($n > 7$)), have attracted tremendous interest since 2008.^[68]

It is known that pillararenes have high affinity toward neutral nitrile moieties. Based on this knowledge, Wang et al.^[69] designed a TPE-functionalized pillar[5]arene (TPEP5) by attaching

four DMPillar[5]arene (DMP5) groups to the periphery of TPE (Figure 29). In $\text{CH}_2\text{Cl}_2/\text{acetone}$ this molecule is nonemissive. However, on addition of the guest molecule (G1), TPEP5 was effectively induced to form spherical aggregates due to the pillararene-based host-guest recognition and resulted in a “turn-on” fluorescence emission.

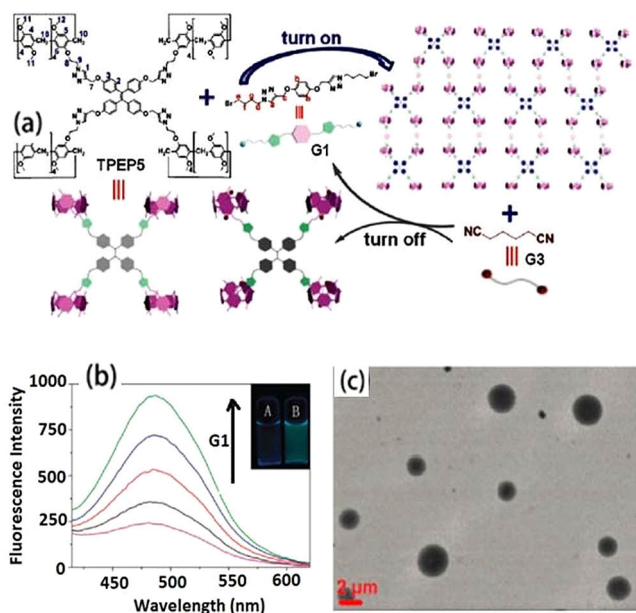


Figure 29. a) Schematic illustration of the assembly of the host-guest recognition complex of TPEP5 and G1.^[69] b) Change in fluorescence with addition of G1 to a solution of TPEP5. c) TEM image of the host-guest complex formed by TPEP5 and G1.

Similar designs were carried out by J. Yang et al.,^[68a] H.-B. Yang et al.,^[70] and Y.-W. Yang et al.^[71] As shown in Figure 30a, the strategy was based on host-guest interactions between the functionalized cationic pillar[5]arene (CWP5-TPE) and sodium dodecyl benzene sulfonate (SDBS). This supramolecular self-assembles in water as nanoparticles, which results in efficient enhancement of the fluorescence. Y.-W. Yang et al.^[71] used a TPE-bridged pillar[5]arene (P5) tetramer, TPE-(P5)₄ (H1), to interact with a triazole-based neutral linker (G2; Figure 30b). This host-guest complex was able to form stimuli-responsive supramolecular gels with strong blue fluorescence.

These pillararene-based AIE supramolecules can be used as chemical sensors. Wu et al.^[72] constructed a new supramolecular system by self-assembly of thymine-substituted copillar[5]arene **1** and TPE derivative **2** in the presence of Hg^{2+} (Figure 31a). Catcher **1** is able to coordinate with Hg^{2+} through thymine to form a linear structure. Furthermore, catcher **1** can bind with indicator **2** through a host-guest interaction to form a crosslinked structure, which eventually wraps into spherical nanoparticles (Figure 31b–c). In solution, the nanoparticles are highly emissive under $\lambda = 365 \text{ nm}$ UV light. After addition of sodium sulfide, catcher **1** and indicator **2** can be recycled. This procedure is aimed at accomplishing the goals of Hg^{2+} sensing and removal in one pot.

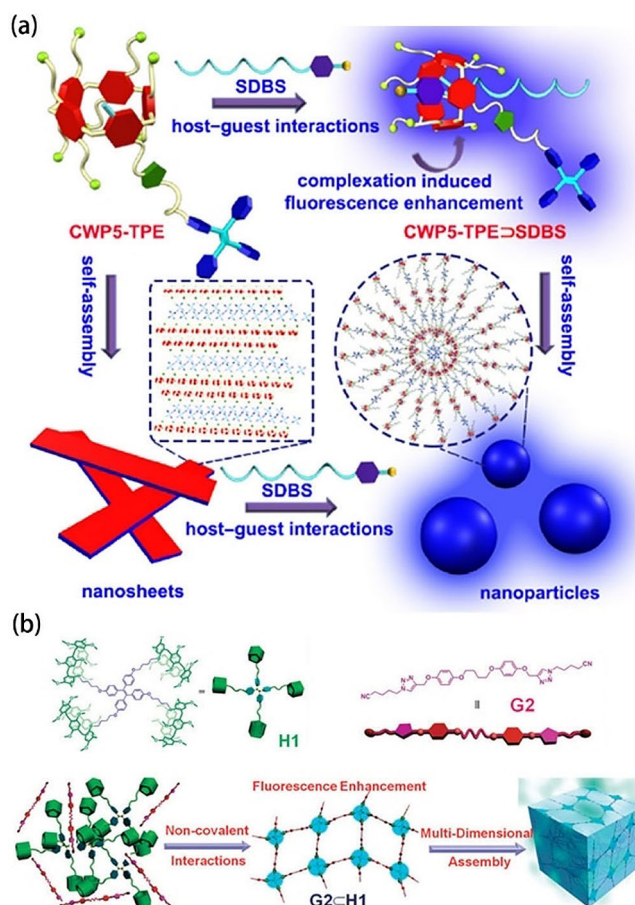


Figure 30. a) Schematic illustration of the self-assembled structures of CWP5-TPE@SDBS.^[68a] b) Schematic illustration of the construction of fluorescent supramolecular polymers of G2@H1.^[71]

Pillar[5]arene-based amphiphilic supramolecular brush copolymers

Huang et al.^[73] constructed a pillararene-based amphiphilic supramolecular brush copolymer, P5-PEG-Biotin@PTPE, which self-assembles into supramolecular nanoparticles. The host-guest recognition between pillar[5]arene (P5) and the 4,4'-bipyridinium derivative (M) is mainly driven by charge transfer and hydrophobic interactions (Figure 32a–b). The complexes were further wrapped into core-shell structured nanoparticles, which may be regarded as a good candidate for encapsulation of the anticancer drug doxorubicin (DOX).

Calix[4]pyrrole-based host-guest chemistry to give luminescent vesicles

Calix structures are another family of host molecules that can be used to construct luminescent molecular self-assemblies based on AIEgens. For example, Sessler et al.^[74] constructed fluorescent molecular self-assembled structures by using water-soluble calix[4]pyrrole and a ditopic pyridine *N*-oxide derivative in water (Figure 33a). The host-guest chemistry between calix[4]pyrrole and the ditopic pyridine *N*-oxide derivative produces a bola-type supra-amphiphile, which further self-assembles

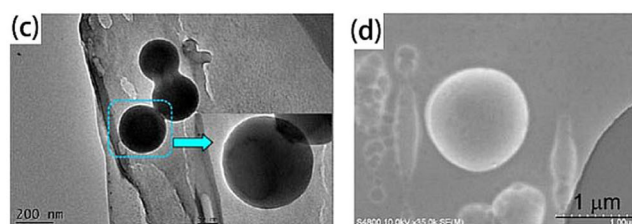
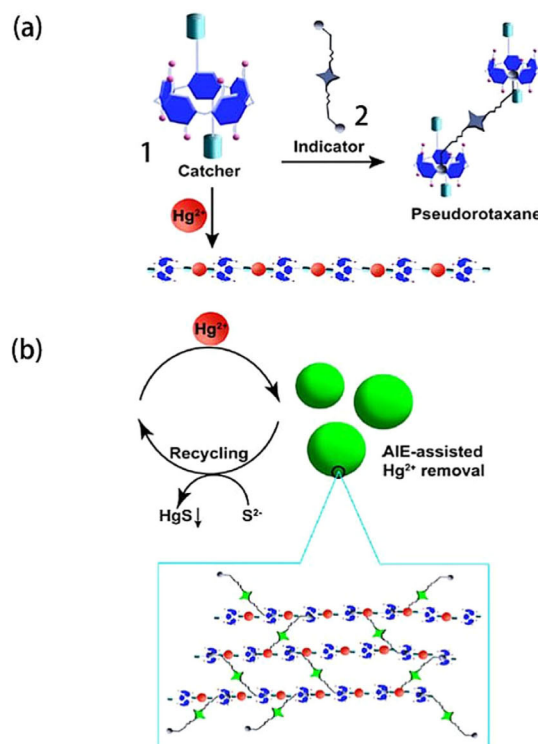


Figure 31. a, b) Schematic illustration of the formation of 2C1@Hg²⁺ nanoparticles. c) TEM and d) SEM images of 2C1@Hg²⁺.^[72]

into multilamellar vesicles and micelles depending on the pH of the solution (Figure 33b–c). The vesicles exhibit strong fluorescence due to restriction of rotation of the TPE moiety embedded in the ditopic pyridine *N*-oxide derivative. The resulting structures may be used to recognize, encapsulate, and release nonfluorescent, water-soluble small molecules.

Luminescent nanoparticle constructed with β-CD through host-guest interactions

Cyclodextrins (CDs) are a classic host able to shelter alkyl chains, benzene rings, and other organic structures of the correct size.^[75] In recent years, CDs have been used to construct supramolecular architectures that can undergo further self-assembly.^[75] When CD and a guest group are covalently attached to a polymer block, a simple combination of the two will lead to the formation of a supramolecular block copolymer.^[76] This strategy was employed by Wei et al. to fabricate an amphiphilic AIE-active copolymer through the specific host-guest interaction between β-CD and an adamantane-terminated TPE derivative (TPE-Ad).^[77] Due to the specific encapsulating effect between adamantane and β-CD, a TPE-β-CD-PEG complex was

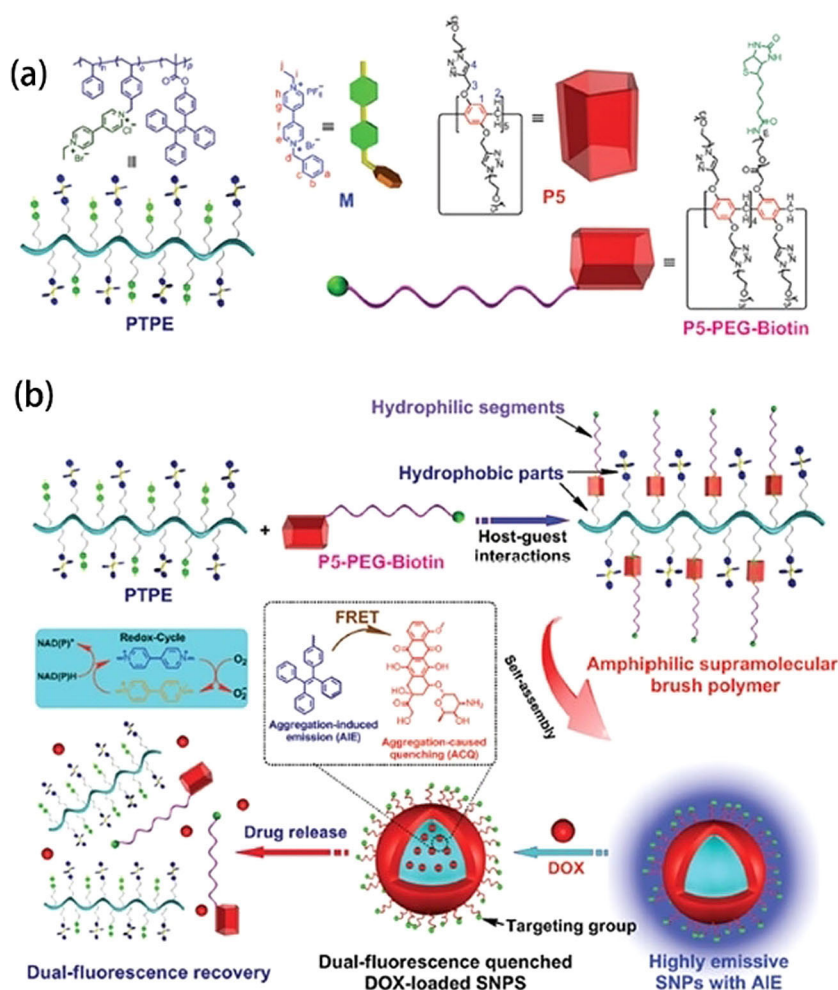


Figure 32. a,b) Schematic illustration of the formation of supramolecular nanoparticles of P5-PEG-Biotin/PTPE.^[73]

formed that was prone to further self-assembly into nanoparticles (Figure 34).

CDs can form intermolecular hydrogen bonds, and these hydrogen bonds can be strengthened when hosting a guest because the host-guest complex as a whole has slower Brownian motion, which is beneficial for hydrogen-bond formation between the CDs.^[78] When TPE is linked directly to cyclodextrins (TPE-CDs), it can self-assemble into nanosheets with hydrophobic TPE layers sandwiched between two hydrophilic cyclodextrin layers^[79] (Figure 35a). This structure can be used to detect organic pollutants, which are collected and transported to the TPE layers. This increases the solubility of TPE and quenches the fluorescence emission.

The macrocyclic compound sulfato- β -cyclodextrin (SCD) is able to induce OPV-I to aggregate into spherical nanoparticles.^[80] The hydrophobic dye NR, which acts as an acceptor, is loaded into the OPV-I/SCD assembly that acts as a donor (Figure 35b). A valid energy transfer can occur and render the system an efficient artificial light-harvesting platform.

Noncovalent-interaction-induced coassembly of AIE-active molecules with other structure-directing molecules

Coassembly is widely employed in the field of molecular self-assembly. Because there are weak interactions between molecules of different types, the addition of another molecule to the target system may result in coassembly of the two.^[81] This strategy is suitable for non- or weakly aggregating AIE molecules. Tang et al. designed a barbituric acid-functionalized tetraphenylethene derivative (TPE-HPh-Bar; Figure 36a), which can self-assemble into nanoparticles upon natural evaporation of its solution^[82] (Figure 36b). In the presence of melamine, nanorods and (un)sealed nanotubes are formed, the ultimate structure depends on the amount of melamine (Figure 36c). The explanation for this phenomenon is that the melamine molecules induce an ordered arrangement of TPE-HPh-Bar through intermolecular hydrogen bonding in certain dimensions. In a similar strategy, Yan et al. reported that formation of the nanoparticles can be tuned by physically mixing TPE-COOH with different short peptides.^[83]

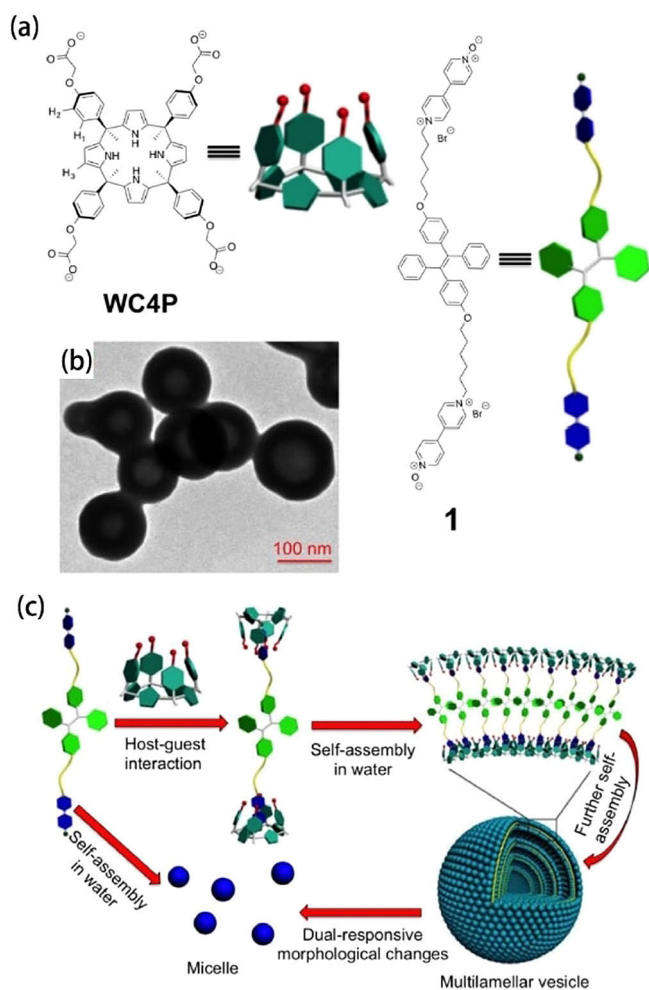


Figure 33. a) Structures of WC4P and 1. b) TEM image of WC4P + 1 aggregates at 25 °C. c) Schematic illustration of the self-assembly of pillarin-based fluorescent vesicles.^[74]

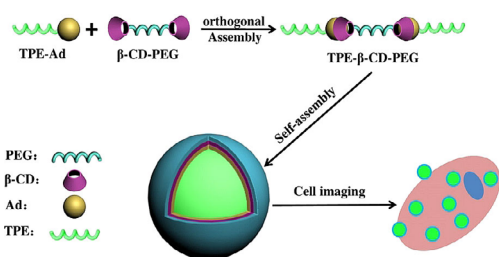


Figure 34. Schematic of the preparation of fluorescent organic nanoparticles (FONs) of TPE-β-CD-PEG.^[77]

Conclusion and Perspectives

The AIE effect no doubt opens a new avenue in material science, which has not only triggered interest in luminescent materials, but also brings about considerations on how to pack them in the desired mode. In contrast to traditional molecules that have very clear packing arrangements and well-recognized noncovalent interactions, the twisted or nonplanar topol-

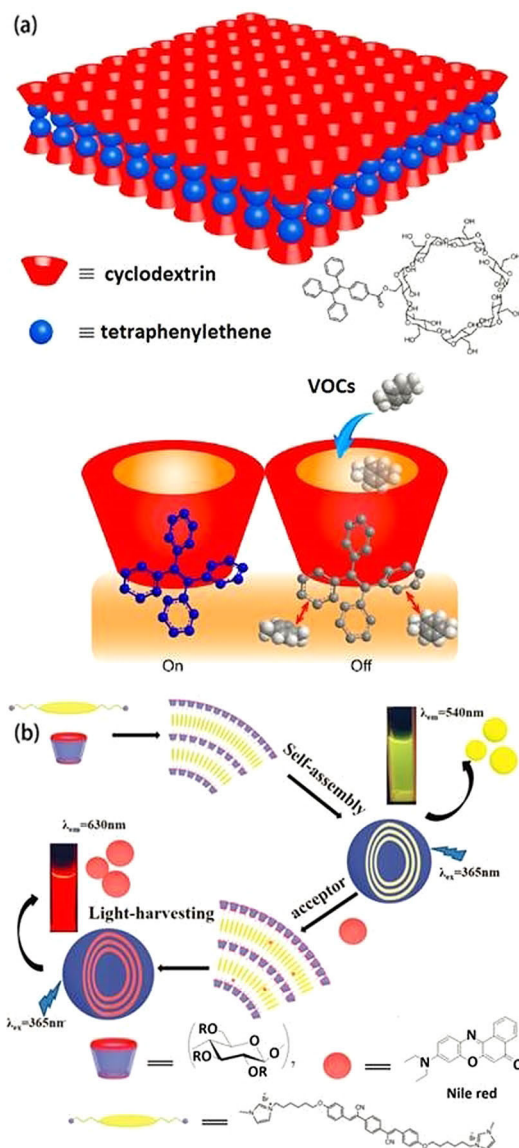


Figure 35. a) Schematic illustration of nanosheets formed by TPE-CDs for VOCs sensing.^[79] b) Construction of a light-harvesting system from OPV-I, SCD, and NR.^[80]

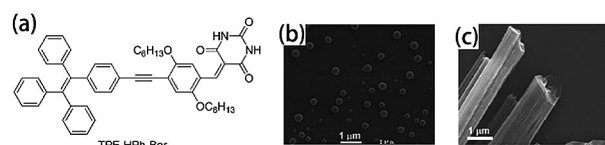


Figure 36. a) Molecular structure of TPE-HPh-Bar. b) SEM image of nanospheres formed by slow evaporation of a solution of TPE-HPh-Bar in acetonitrile (10 μm). c) SEM image of nanoaggregates formed by slow evaporation of TPE-HPh-Bar (10 μm) in DMSO/ethanol (1:1 v/v) at RT in the presence of melamine (10 equiv).^[82]

ogy of AIEgens makes it difficult to understand their intermolecular interactions. Although herein we have summarized progress in the self-assembly of AIE molecules, deeper physical insight into their packing mechanisms is still not sufficient. We

believe that dipole interactions and van der Waals forces play significant roles in their self-assembly and aggregation.

Furthermore, the mechanism behind the solvent effect on the self-assembly behavior of this class of molecules is not clear. To date, it seems that the solvent polarity and dielectric constant may affect the electronic state of the AIE molecules because the rotatory ability and the conjugated status of these molecules can be highly influenced by these solvent parameters. In the future, we expect the intermolecular interactions between AIE molecules will attract more sophisticated studies, which will lay the foundation for precise control over the self-assembly behavior of AIE molecules through molecular design and supramolecular pathways. We believe that well-designed self-assembling AIE systems will bring intriguing functions to materials science, biology, pharmacy, information, and other high-tech fields.

Acknowledgements

This work was financially supported by the National Natural Science Foundation of China (NSFC, grant nos. 91856120, 21573011, 21633002) and the Ministry of Science and Technology of China (2017YFB0308800).

Conflict of interest

The authors declare no conflict of interest.

Keywords: aggregation-induced emission • amphiphiles • noncovalent interactions • polymers • self-assembly

- [1] a) H. Wang, X. Ji, Z. Li, F. Huang, *Adv. Mater.* **2017**, *29*, 1606117; b) Z. W. Wang, J. J. Qiu, X. S. Wang, Z. P. Zhang, Y. H. Chen, X. Huang, W. Huang, *Chem. Soc. Rev.* **2018**, *47*, 6128–6174; c) M. R. Zhu, C. L. Yang, *Chem. Soc. Rev.* **2013**, *42*, 4963–4976; d) H. Gao, X. Zhang, C. Chen, K. Li, D. Ding, *Adv. Biosyst.* **2018**, *2*, 1800074; e) J. Qi, C. Chen, D. Ding, B. Z. Tang, *Adv. Healthcare Mater.* **2018**, *7*, 1800477.
- [2] J. Wang, Y. Zhao, C. Dou, H. Sun, P. Xu, K. Ye, J. Zhang, S. Jiang, F. Li, Y. Wang, *J. Phys. Chem. B* **2007**, *111*, 5082–5089.
- [3] S. H. Lee, B.-B. Jang, Z. H. Kafafi, *J. Am. Chem. Soc.* **2005**, *127*, 9071–9078.
- [4] J. Luo, Z. Xie, J. W. Y. Lam, L. Cheng, B. Z. Tang, H. Chen, C. Qiu, H. S. Kwok, X. Zhan, Y. Liu, D. Zhu, *Chem. Commun.* **2001**, 1740–1741.
- [5] L. Q. Yan, Z. N. Kong, Y. Xia, Z. J. Qi, *New J. Chem.* **2016**, *40*, 7061–7067.
- [6] M. Gao, B. Z. Tang, *ACS Sens.* **2017**, *2*, 1382–1399.
- [7] Y. Yan, J. Huang, B. Z. Tang, *Chem. Commun.* **2016**, *52*, 11870–11884.
- [8] H. Li, X. Zheng, H. Su, J. W. Lam, K. Sing Wong, S. Xue, X. Huang, X. Huang, B. S. Li, B. Z. Tang, *Sci. Rep.* **2016**, *6*, 19277.
- [9] J. Mei, N. L. C. Leung, R. T. K. Kwok, J. W. Y. Lam, B. Z. Tang, *Chem. Rev.* **2015**, *115*, 11718–11940.
- [10] a) Y. Yan, W. Xiong, J. B. Huang, Z. C. Li, X. S. Li, N. N. Li, H. L. Fu, *J. Phys. Chem. B* **2005**, *109*, 357–364; b) Y. Yan, J. B. Huang, Z. C. Li, J. M. Ma, H. L. Fu, J. P. Ye, *J. Phys. Chem. B* **2003**, *107*, 1479–1482; c) Y. Yan, J. B. Huang, Z. C. Li, F. Han, J. M. Ma, *Langmuir* **2003**, *19*, 972–974.
- [11] a) Anuradha, D. D. La, M. Al Kobaisi, S. V. Bhosale, *Sci. Rep.* **2015**, *5*, 15652; b) Anuradha, D. D. La, M. A. Kobaisi, A. Gupta, S. V. Bhosale, *Chem. Eur. J.* **2017**, *23*, 3950–3956.
- [12] Y. Xia, L. Dong, Y. Jin, S. Wang, L. Yan, S. Yin, S. Zhou, B. Song, *J. Mater. Chem. B* **2015**, *3*, 491–497.
- [13] N. Li, Y. Y. Liu, Y. Li, J. B. Zhuang, R. R. Cui, Q. Gong, N. Zhao, B. Z. Tang, *ACS Appl. Mater. Interfaces* **2018**, *10*, 24249–24257.
- [14] M. Zhang, X. Yin, T. Tian, Y. Liang, W. Li, Y. Lan, J. Li, M. Zhou, Y. Ju, G. Li, *Chem. Commun.* **2015**, *51*, 10210–10213.
- [15] H. Huang, M. Liu, S. Luo, K. Wang, Q. Wan, F. Deng, D. Xu, X. Zhang, Y. Wei, *Chem. Eng. J.* **2016**, *304*, 149–155.
- [16] a) X. Zhang, X. Zhang, B. Yang, J. Hui, M. Liu, Z. Chi, S. Liu, J. Xu, Y. Wei, *Polym. Chem.* **2014**, *5*, 318–322; b) Y. L. Jin, X. D. Zhang, *Linear Algebra Appl.* **2014**, *448*, 285–291; c) X. L. Zhang, Z. F. Cheng, S. Y. Hou, G. Zhuang, J. Luo, *Rev. Sci. Instrum.* **2014**, *85*, 11E420; d) Y. Wu, L. Qu, J. Li, L. Huang, Z. Liu, *Polymer* **2018**, *158*, 297–307.
- [17] a) X. Zhang, X. Zhang, B. Yang, M. Liu, W. Liu, Y. Chen, Y. Wei, *Polym. Chem.* **2013**, *4*, 4317; b) Q. Wan, M. Liu, D. Xu, H. Huang, L. Mao, G. Zeng, F. Deng, X. Zhang, Y. Wei, *J. Mater. Chem. B* **2016**, *4*, 4033–4039.
- [18] X. Zhang, X. Zhang, B. Yang, Y. Yang, Y. Wei, *Polym. Chem.* **2014**, *5*, 5885–5889.
- [19] a) X. Zhang, X. Zhang, B. Yang, M. Liu, W. Liu, Y. Chen, Y. Wei, *Polym. Chem.* **2014**, *5*, 356–360; b) X. Zhang, M. Liu, B. Yang, X. Zhang, Z. Chi, S. Liu, J. Xu, Y. Wei, *Polym. Chem.* **2013**, *4*, 5060.
- [20] X. Zhang, X. Zhang, B. Yang, M. Liu, W. Liu, Y. Chen, Y. Wei, *Polym. Chem.* **2014**, *5*, 399–404.
- [21] X. Zhang, X. Zhang, B. Yang, J. Hui, M. Liu, Z. Chi, S. Liu, J. Xu, Y. Wei, *Polym. Chem.* **2014**, *5*, 683–688.
- [22] C. Zhang, S. Jin, S. Li, X. Xue, J. Liu, Y. Huang, Y. Jiang, W. Q. Chen, G. Zou, X. J. Liang, *ACS Appl. Mater. Interfaces* **2014**, *6*, 5212–5220.
- [23] a) Y. Zhang, Y. Chen, X. Li, J. Zhang, J. Chen, B. Xu, X. Fu, W. Tian, *Polym. Chem.* **2014**, *5*, 3824–3830; b) A. Han, H. Wang, R. T. Kwok, S. Ji, J. Li, D. Kong, B. Z. Tang, B. Liu, Z. Yang, D. Ding, *Anal. Chem.* **2016**, *88*, 3872–3878.
- [24] a) H. Li, X. Zhang, X. Zhang, B. Yang, Y. Yang, Y. Wei, *Polym. Chem.* **2014**, *5*, 3758; b) R. Jiang, M. Cao, M. Liu, L. Liu, Q. Huang, H. Huang, Y. Wen, Q. Y. Cao, X. Zhang, Y. Wei, *Mater. Sci. Eng. C* **2018**, *92*, 61–68; c) Y. Liu, L. Mao, S. Yang, M. Liu, H. Huang, Y. Wen, F. Deng, Y. Li, X. Zhang, Y. Wei, *Mater. Sci. Eng. C* **2019**, *94*, 310–317; d) X. Guan, B. Lu, Q. Jin, Z. Li, L. Wang, K. Wang, S. Lai, Z. Lei, *Ind. Eng. Chem. Res.* **2018**, *57*, 14889–14898.
- [25] Y. Zhang, C. X. Wang, S. W. Huang, *Nanomaterials* **2018**, *8*, 921.
- [26] W. Chen, G. Qing, T. Sun, *Chem. Commun.* **2017**, *53*, 447–450.
- [27] a) H. Wang, C. Ren, Z. Song, L. Wang, X. Chen, Z. Yang, *Nanotechnology* **2010**, *21*, 225606; b) Y. Zhang, N. Zhou, S. Akella, Y. Kuang, D. Kim, A. Schwartz, M. Bezpalko, B. M. Foxman, S. Fraden, I. R. Epstein, B. Xu, *Angew. Chem. Int. Ed.* **2013**, *52*, 11494–11498; *Angew. Chem.* **2013**, *125*, 11708–11712; c) H. Wang, C. Yang, M. Tan, L. Wang, D. Kong, Z. Yang, *Soft Matter* **2011**, *7*, 3897.
- [28] X. M. Liu, G. L. Liang, *Chem. Commun.* **2017**, *53*, 1037–1040.
- [29] H. Frisch, D. Spitzer, M. Haase, T. Basche, J. Voskuhl, P. Besenius, *Org. Biomol. Chem.* **2016**, *14*, 5574–5579.
- [30] a) H. Li, J. Cheng, Y. Zhao, J. W. Y. Lam, K. S. Wong, H. Wu, B. S. Li, B. Z. Tang, *Mater. Horiz.* **2014**, *1*, 518–521; b) H. Li, J. Cheng, H. Deng, E. Zhao, B. Shen, J. W. Y. Lam, K. S. Wong, H. Wu, B. S. Li, B. Z. Tang, *J. Mater. Chem. C* **2015**, *3*, 2399–2404.
- [31] J. Liu, H. Su, L. Meng, Y. Zhao, C. Deng, J. C. Y. Ng, P. Lu, M. Faisal, J. W. Y. Lam, X. Huang, H. Wu, K. S. Wong, B. Z. Tang, *Chem. Sci.* **2012**, *3*, 2737.
- [32] Z. Zhao, S. Chen, X. Shen, F. Mahtab, Y. Yu, P. Lu, J. W. Lam, H. S. Kwok, B. Z. Tang, *Chem. Commun.* **2010**, *46*, 686–688.
- [33] H. Zhou, J. Li, M. H. Chua, H. Yan, Q. Ye, J. Song, T. T. Lin, B. Z. Tang, J. Xu, *Chem. Commun.* **2016**, *52*, 12478–12481.
- [34] W. Z. Yuan, F. Mahtab, Y. Gong, Z.-Q. Yu, P. Lu, Y. Tang, J. W. Y. Lam, C. Zhu, B. Z. Tang, *J. Mater. Chem.* **2012**, *22*, 10472.
- [35] D. Bele, C. Dumea, E. Bicu, L. Marin, *RSC Adv.* **2015**, *5*, 8849–8858.
- [36] A. Rananaware, R. S. Bhosale, K. Ohkubo, H. Patil, L. A. Jones, S. L. Jackson, S. Fukuzumi, S. V. Bhosale, S. V. Bhosale, *J. Org. Chem.* **2015**, *80*, 3832–3840.
- [37] A. Rananaware, R. S. Bhosale, H. Patil, M. Al Kobaisi, A. Abraham, R. Shukla, S. V. Bhosale, S. V. Bhosale, *RSC Adv.* **2014**, *4*, 59078–59082.
- [38] W. Han, S. Zhang, J. Qian, J. Zhang, X. Wang, Z. Xie, B. Xu, Y. Han, W. Tian, *Chem. Asian J.* **2018**, DOI: 10.1002/asia.201801527.
- [39] R. Hu, J. W. Y. Lam, H. Deng, Z. Song, C. Zheng, B. Z. Tang, *J. Mater. Chem. C* **2014**, *2*, 6326–6332.
- [40] C. Shi, Z. Guo, Y. Yan, S. Zhu, Y. Xie, Y. S. Zhao, W. Zhu, H. Tian, *ACS Appl. Mater. Interfaces* **2013**, *5*, 192–198.
- [41] a) Y. Hou, J. R. Du, J. D. Hou, P. J. Shi, T. Y. Han, Y. A. Duan, *J. Lumin.* **2018**, *204*, 221–229; b) J. Y. Sun, J. Yuan, Y. P. Li, Y. Duan, Z. F. Li, J. R.

- Du, T. Y. Han, *Sens. Actuators B* **2018**, *263*, 208–217; c) J. Q. Han, Y. P. Li, J. Yuan, Z. F. Li, R. X. Zhao, T. Y. Han, T. D. Han, *Sens. Actuators B* **2018**, *258*, 373–380; d) T. Y. Han, W. Wei, J. Yuan, Y. Duan, Y. P. Li, L. Y. Hu, Y. P. Dong, *Talanta* **2016**, *150*, 104–112.
- [42] C. Niu, L. Zhao, T. Fang, X. Deng, H. Ma, J. Zhang, N. Na, J. Han, J. Ouyang, *Langmuir* **2014**, *30*, 2351–2359.
- [43] X. Y. Shen, Y. J. Wang, E. Zhao, W. Z. Yuan, Y. Liu, P. Lu, A. Qin, Y. Ma, J. Z. Sun, B. Z. Tang, *J. Phys. Chem. C* **2013**, *117*, 7334–7347.
- [44] Y. Zang, Y. Li, B. Li, H. Li, Y. Yang, *RSC Adv.* **2015**, *5*, 38690–38695.
- [45] P. Galer, R. C. Korosec, M. Vidmar, B. Sket, *J. Am. Chem. Soc.* **2014**, *136*, 7383–7394.
- [46] B. Xu, J. He, Y. Dong, F. Chen, W. Yu, W. Tian, *Chem. Commun.* **2011**, *47*, 6602–6604.
- [47] I. Javed, T. Zhou, F. Muhammad, J. Guo, H. Zhang, Y. Wang, *Langmuir* **2012**, *28*, 1439–1446.
- [48] a) Y. T. Kang, X. Y. Tang, Z. G. Cai, X. Zhang, *Adv. Funct. Mater.* **2016**, *26*, 8920–8931; b) Y. T. Kang, K. Liu, X. Zhang, *Langmuir* **2014**, *30*, 5989–6001; c) C. Wang, Z. Q. Wang, X. Zhang, *Acc. Chem. Res.* **2012**, *45*, 608–618.
- [49] X. Yan, H. Wang, C. E. Hauke, T. R. Cook, M. Wang, M. L. Saha, Z. Zhou, M. Zhang, X. Li, F. Huang, P. J. Stang, *J. Am. Chem. Soc.* **2015**, *137*, 15276–15286.
- [50] a) H. T. Feng, Y. X. Yuan, J. B. Xiong, Y. S. Zheng, B. Z. Tang, *Chem. Soc. Rev.* **2018**, *47*, 7452–7476; b) X.-Y. Lou, Y.-W. Yang, *Adv. Opt. Mater.* **2018**, *6*, 1800668.
- [51] C. F. J. Faul, M. Antonietti, *Adv. Mater.* **2003**, *15*, 673–683.
- [52] a) H. Jing, L. Lu, Y. Feng, J.-F. Zheng, L. Deng, E.-Q. Chen, X.-K. Ren, *J. Phys. Chem. C* **2016**, *120*, 27577–27586; b) C. F. J. Faul, *Acc. Chem. Res.* **2014**, *47*, 3428–3438.
- [53] J. Li, K. Liu, H. Chen, R. Li, M. Drechsler, F. Bai, J. Huang, B. Z. Tang, Y. Yan, *ACS Appl. Mater. Interfaces* **2017**, *9*, 21706–21714.
- [54] J. Li, K. J. Shi, M. Drechsler, B. Z. Tang, J. B. Huang, Y. Yan, *Chem. Commun.* **2016**, *52*, 12466–12469.
- [55] J. Li, K. Liu, Y. Han, B. Z. Tang, J. Huang, Y. Yan, *ACS Appl. Mater. Interfaces* **2016**, *8*, 27987–27995.
- [56] a) D. Zhao, F. Fan, J. Cheng, Y. Zhang, K. S. Wong, V. G. Chigrinov, H. S. Kwok, L. Guo, B. Z. Tang, *Adv. Opt. Mater.* **2015**, *3*, 199–202; b) W. Z. Yuan, Z.-Q. Yu, P. Lu, C. Deng, J. W. Y. Lam, Z. Wang, E.-Q. Chen, Y. Ma, B. Z. Tang, *J. Mater. Chem.* **2012**, *22*, 3323; c) W. Z. Yuan, Z.-Q. Yu, Y. Tang, J. W. Y. Lam, N. Xie, P. Lu, E.-Q. Chen, B. Z. Tang, *Macromolecules* **2011**, *44*, 9618–9628; d) S.-J. Yoon, J. H. Kim, K. S. Kim, J. W. Chung, B. Heinrich, F. Mathevet, P. Kim, B. Donnio, A.-J. Attias, D. Kim, S. Y. Park, *Adv. Funct. Mater.* **2012**, *22*, 61–69; e) Y. Ren, W. H. Kan, M. A. Henderson, P. G. Bomben, C. P. Berlinguette, V. Thangadurai, T. Baumgartner, *J. Am. Chem. Soc.* **2011**, *133*, 17014–17026; f) H. Lu, L. Qiu, G. Zhang, A. Ding, W. Xu, G. Zhang, X. Wang, L. Kong, Y. Tian, J. Yang, *J. Mater. Chem. C* **2014**, *2*, 1386; g) J. W. Park, S. Nagano, S.-J. Yoon, T. Dohi, J. Seo, T. Seki, S. Y. Park, *Adv. Mater.* **2014**, *26*, 1354–1359; h) Q. Ye, D. Zhu, L. Xu, X. Lu, Q. Lu, *J. Mater. Chem. C* **2016**, *4*, 1497–1503.
- [57] C. Wang, Y. S. Guo, Z. Q. Wang, X. Zhang, *Langmuir* **2010**, *26*, 14509–14511.
- [58] G. Yu, G. Tang, F. Huang, *J. Mater. Chem. C* **2014**, *2*, 6609–6617.
- [59] a) M. Zhang, M. L. Saha, M. Wang, Z. Zhou, B. Song, C. Lu, X. Yan, X. Li, F. Huang, S. Yin, P. J. Stang, *J. Am. Chem. Soc.* **2017**, *139*, 5067–5074; b) X. D. Gao, Y. J. Wang, X. L. Wang, X. F. Guo, J. B. Huang, Y. Yan, *J. Mater. Chem. C* **2017**, *5*, 8936–8943; c) Y. J. Wang, X. D. Gao, Y. L. Xiao, Q. Zhao, J. Yang, Y. Yan, J. B. Huang, *Soft Matter* **2015**, *11*, 2806–2811; d) Y. Yan, J. B. Huang, *Coord. Chem. Rev.* **2010**, *254*, 1072–1080.
- [60] G. Kumar, R. Gupta, *Chem. Soc. Rev.* **2013**, *42*, 9403–9453.
- [61] L. M. Xu, L. X. Jiang, M. Drechsler, Y. Sun, Z. R. Liu, J. B. Huang, B. Z. Tang, Z. B. Li, M. A. C. Stuart, Y. Yan, *J. Am. Chem. Soc.* **2014**, *136*, 1942–1947.
- [62] G. Q. Yin, H. Wang, X. Q. Wang, B. Song, L. J. Chen, L. Wang, X. Q. Hao, H. B. Yang, X. Li, *Nat. Commun.* **2018**, *9*, 567.
- [63] H.-T. Feng, S. Song, Y.-C. Chen, C.-H. Shen, Y.-S. Zheng, *J. Mater. Chem. C* **2014**, *2*, 2353–2359.
- [64] B. Liu, H. Zhou, B. Yang, X. Hu, *Sens. Actuators B* **2017**, *246*, 554–562.
- [65] a) C. Lu, M. Zhang, D. Tang, X. Yan, Z. Zhang, Z. Zhou, B. Song, H. Wang, X. Li, S. Yin, H. Sepehrpour, P. J. Stang, *J. Am. Chem. Soc.* **2018**, *140*, 7674–7680; b) X. Yan, T. R. Cook, P. Wang, F. Huang, P. J. Stang, *Nat. Chem.* **2015**, *7*, 342–348; c) Z. Zhou, X. Yan, M. L. Saha, M. Zhang, M. Wang, X. Li, P. J. Stang, *J. Am. Chem. Soc.* **2016**, *138*, 13131–13134; d) Y. L. Chen, Y. Y. Zhang, Q. W. Cheng, M. Y. Niu, H. Z. Liang, H. F. Yan, X. H. Zhang, J. A. T. da Silva, G. H. Ma, *In Vitro Cell. Dev. Biol. Plant* **2016**, *52*, 521–529.
- [66] L. J. Chen, Y. Y. Ren, N. W. Wu, B. Sun, J. Q. Ma, L. Zhang, H. Tan, M. Liu, X. Li, H. B. Yang, *J. Am. Chem. Soc.* **2015**, *137*, 11725–11735.
- [67] G. Yu, M. Zhang, M. L. Saha, Z. Mao, J. Chen, Y. Yao, Z. Zhou, Y. Liu, C. Gao, F. Huang, X. Chen, P. J. Stang, *J. Am. Chem. Soc.* **2017**, *139*, 15940–15949.
- [68] a) J. Sun, L. Shao, J. Zhou, B. Hua, Z. Zhang, Q. Li, J. Yang, *Tetrahedron Lett.* **2018**, *59*, 147–150; b) T. Ogoishi, S. Kanai, S. Fujinami, T.-a. Yamagishi, Y. Nakamoto, *J. Am. Chem. Soc.* **2008**, *130*, 5022–5023.
- [69] J. Wu, S. Sun, X. Feng, J. Shi, X. Y. Hu, L. Wang, *Chem. Commun.* **2014**, *50*, 9122–9125.
- [70] C.-W. Zhang, S.-T. Jiang, G.-Q. Yin, X. Li, X.-L. Zhao, H.-B. Yang, *Isr. J. Chem.* **2018**, *58*, 1265–1272.
- [71] N. Song, D. X. Chen, Y. C. Qiu, X. Y. Yang, B. Xu, W. Tian, Y. W. Yang, *Chem. Commun.* **2014**, *50*, 8231–8234.
- [72] H. B. Cheng, Z. Li, Y. D. Huang, L. Liu, H. C. Wu, *ACS Appl. Mater. Interfaces* **2017**, *9*, 11889–11894.
- [73] G. Yu, R. Zhao, D. Wu, F. Zhang, L. Shao, J. Zhou, J. Yang, G. Tang, X. Chen, F. Huang, *Polym. Chem.* **2016**, *7*, 6178–6188.
- [74] X. Chi, H. Zhang, G. I. Vargas-Zuniga, G. M. Peters, J. L. Sessler, *J. Am. Chem. Soc.* **2016**, *138*, 5829–5832.
- [75] Y. Yan, L. X. Jiang, J. B. Huang, *Phys. Chem. Chem. Phys.* **2011**, *13*, 9074–9082.
- [76] Z. K. Du, K. Ke, X. Y. Chang, R. F. Dong, B. Y. Ren, *Langmuir* **2018**, *34*, 5606–5614.
- [77] H. Huang, D. Xu, M. Liu, R. Jiang, L. Mao, Q. Huang, Q. Wan, Y. Wen, X. Zhang, Y. Wei, *Mater. Sci. Eng. C* **2017**, *78*, 862–867.
- [78] a) C. C. Zhou, J. B. Huang, Y. Yan, *Soft Matter* **2016**, *12*, 1579–1585; b) C. C. Zhou, X. H. Cheng, Q. Zhao, Y. Yan, J. D. Wang, J. B. Huang, *Sci. Rep.* **2014**, *4*, 7533; c) C. C. Zhou, X. H. Cheng, Y. Yan, J. D. Wang, J. B. Huang, *Langmuir* **2014**, *30*, 3381–3386; d) C. C. Zhou, X. H. Cheng, Q. Zhao, Y. Yan, J. D. Wang, J. B. Huang, *Langmuir* **2013**, *29*, 13175–13182.
- [79] G. Liang, F. Ren, H. Gao, Q. Wu, F. Zhu, B. Z. Tang, *ACS Sens.* **2016**, *1*, 1272–1278.
- [80] J. J. Li, Y. Chen, J. Yu, N. Cheng, Y. Liu, *Adv. Mater.* **2017**, *29*, 1701905.
- [81] a) X. Gu, J. Yao, G. Zhang, D. Zhang, *Small* **2012**, *8*, 3406–3411; b) S. Liu, L. Zhao, Y. Yan, J. B. Huang, *Soft Matter* **2015**, *11*, 2752–2757.
- [82] E. Wang, J. W. Y. Lam, R. Hu, C. Zhang, Y. S. Zhao, B. Z. Tang, *J. Mater. Chem. C* **2014**, *2*, 1801.
- [83] K. Liu, R. Zhang, Y. Li, T. Jiao, D. Ding, X. Yan, *Adv. Mater. Interfaces* **2017**, *4*, 1600183.

Manuscript received: December 19, 2018

Revised manuscript received: January 30, 2019

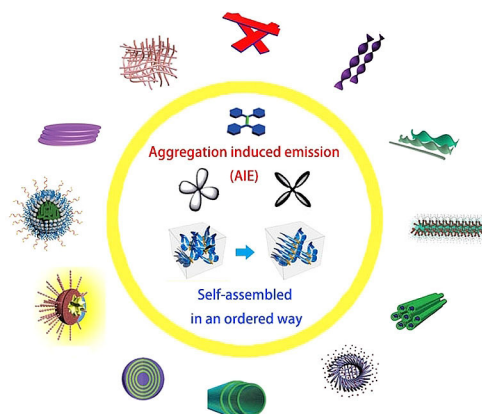
Version of record online: ■■■ 0000

MINIREVIEW

Tongyue Wu, Jianbin Huang, Yun Yan*

■ ■ - ■ ■

Self-Assembly of Aggregation-Induced-Emission Molecules



AIEgens assemble! The nonplanar topology of AIEgens makes it difficult for them to self-assemble into well-defined structures. However, by using appropri-

ate covalent molecular design and non-covalent supramolecular interactions, the elegant self-assembly of AIEgens can be achieved too.